

“Critical Clusters” in a Supersaturated Vapor: Theory and Monte Carlo Simulation

K. Binder¹ and M. H. Kalos²

Received July 2, 1979

A new thermodynamic analysis is given for the equilibrium between a liquid cluster and the surrounding supersaturated gas phase in a *finite* constant volume. It is shown that for constant total density and intermediate volume this equilibrium is stable, although it is unstable for very large volume. We show that observation of the critical cluster size l^* then yields information on the surface free energy of the liquid cluster. The accuracy of previous approximate prescriptions for obtaining the free energy of physical clusters is investigated. As an application, the theory is used to analyze Monte Carlo simulations of the two-dimensional lattice gas model at low temperatures. We obtain cluster surface area, diffusivity, and free energy for clusters with $26 \leq l \leq 500$. It is found that the capillarity approximation is inaccurate for $l \leq 100$, but the free energy of small clusters is *higher* than the result of classical nucleation theory, in contrast to what one expects from Tolman-like corrections. We interpret these results, deriving low-temperature series expansions for very small clusters, thus showing that the capillarity approximation both underestimates the surface energy and overestimates the surface entropy of very small clusters. Finally, we use our results to give a speculative explanation of recent nucleation experiments. The dependence of the cluster diffusivity on cluster size is tentatively explained in terms of a crossover between two mechanisms yielding different power laws.

KEY WORDS : Nucleation ; cluster diffusion ; lattice gas ; computer simulation ; critical cluster ; binary alloy.

1. INTRODUCTION

Calculation of the transformation rate of unstable (or metastable) phases via the nucleation mechanism is an important problem in many branches of physics and chemistry.⁽¹⁻⁵⁾ Although the concepts of this theory are now

Supported by the U.S. Department of Energy under Contract No. EY-76-C-02-3077*000.

¹ IFF, KFA Jülich, Jülich, West Germany.

² Courant Institute of Mathematical Sciences, New York University, New York, N.Y.

fairly well understood in the framework of more general considerations of statistical mechanics, applications of the theory still suffer from the lack of knowledge on the free energy of formation of small "clusters" of the new phase. The standard procedure ("classical nucleation theory") is to apply an extrapolation using the surface tension between macroscopic bulk phases to calculate the surface free energy of very small clusters, the so-called "capillarity approximation."⁽¹⁻⁴⁾ It turns out that this simple model accounts fairly well for many experiments at rather low temperatures (e.g., Refs. 6 and 7), while it fails to describe nucleation in the region near the critical point (e.g., Refs. 8 and 9), where the predicted nucleation rates are by far too high. These findings are surprising for several reasons: (i) At low temperatures the "critical clusters" contain only about 10–1000 molecules, while they contain 10^4 – 10^6 molecules near the critical point. Thus one expects a macroscopic extrapolation to hold in the latter temperature region rather than in the former. (ii) "Thermodynamic" arguments suggest that the surface tension of a small drop depends significantly on its radius of curvature, and predict that the surface free energy of small clusters is distinctly lower than that which would follow from the capillarity approximation ("Tolman correction"⁽¹⁰⁻¹²⁾). (iii) Inclusion of rotation and translation of the droplet distinctly decreases the free energy barrier for the formation of small droplets ("Lothe–Pound correction"^(13,14) in comparison with that of the classical theory. Both corrections imply that the nucleation rates should be much higher than actually observed. (iv) Use of a smooth density profile for the droplets, which follows from a Ginzburg–Landau equation for the nonuniform density, also leads to a decrease of the barrier (Cahn–Hilliard theory⁽¹⁵⁾ and variants thereof^(16,17)).

Clearly, it is very questionable that an extrapolation in terms of the surface tension between macroscopic phases is applicable for clusters of 10–1000 molecules, and all these corrections may be misleading since one needs a "microscopic surface tension" for these small clusters.⁽¹⁸⁾ But the use of the Fisher droplet model⁽¹⁹⁾ suggested by Kiang *et al.*^(18,20) to determine this microscopic surface tension either by a fit to critical point parameters⁽¹⁸⁾ or a fit to the second virial coefficient⁽²¹⁾ has also been shown to be a procedure generally inaccurate (see, e.g., Appendix A of Ref. 5).

A more rigorous treatment was given by Gillis *et al.*⁽²²⁾ for a one-dimensional model. Since one-dimensional fluids with short-range forces do not possess a nonzero gas–fluid critical point, no supersaturated one-dimensional vapor exists. Also, cluster "shapes" in one dimension are very restricted, and hence the extrapolation of these results to higher dimensionality is delicate. In the absence of any theories by which the properties of higher dimensional clusters containing 10–1000 molecules can be calculated from first principles, computer techniques are clearly very valuable to obtain

these properties numerically. However, the many calculations of microcrystallite clusters (see, e.g., Refs. 2, 4, and 23 and references therein) again are reliable only at rather low temperatures, since the configurational entropy must be taken into account.⁽²⁴⁾ In order to account for the latter, which is produced by fluctuations in the precise microscopic structure and shape of the cluster, one has to compute cluster properties from a simulation where the cluster is put into a larger surrounding box, without prescribing a definite structure and shape for the cluster. Such simulations have been done by a variety of authors,⁽²⁵⁻³¹⁾ but several problems remain:

(i) Counting of clusters which form spontaneously due to fluctuations in equilibrium states⁽²⁵⁾ yields useful results only for temperatures close to the critical point and for high supersaturations.

(ii) Simulation of clusters with varying shape but precisely fixed cluster size l and constant thermodynamic variables⁽²⁶⁾ does not yield *direct* information on the free energy barrier (thus the free energy is obtained only by recording the energy over a range of variables up to some reference state, and performing suitable integrations).

(iii) Simulations where all molecules within the box are counted as being part of the cluster^(4,27-29) may be unreliable,⁽³⁰⁾ since rather disconnected configurations which physically would correspond to several clusters are regarded as just one cluster. In addition, there is always some residual dependence of the cluster free energy on the size of the box, which has not yet been analyzed in sufficient detail. Thus it sometimes may be hard to judge the accuracy of these simulations, and it is not surprising that the discrepancies between recent Monte Carlo⁽²⁸⁾ and molecular dynamics⁽²⁹⁾ simulations are beyond the respective quoted error bars.

The purpose of the present work is now twofold: First we give an analysis of the equilibrium of a cluster with the surrounding gas in a box of finite size (Section 2). The conditions are obtained under which this equilibrium is thermodynamically stable. It is shown that one can obtain information on the surface free energy of the cluster independent of the size of the box. In Section 3 we use this treatment to estimate the order of the approximation which results from the treatment cited in (iii) above, where all molecules within the box are counted as being part of the cluster. In Section 4 we show that our theory actually presents the basis for practical analysis of computer simulations, studying clusters of up to about 500 atoms in the two-dimensional lattice gas model, where stochastic interchanges of the occupation number of neighboring sites are performed. While this study is thus not immediately applicable to any real system, apart from clustering of atoms at planar surfaces, where our kinetics models surface diffusion,⁽³²⁾ the model has distinct advantages for our purposes: (i) Both the chemical potential at the coexistence curve and the surface tension are known unambiguously, from

Onsager's solution.⁽³³⁾ The existing, albeit small, uncertainties in the numerical values of both quantities for the more interesting Lennard-Jones fluids have a nonnegligible effect for clusters with critical sizes l^* from 100 to 1000, of course, and thus make a reliable estimation of correction terms difficult. (ii) Due to the absence of degrees of freedom for any inertial motion in the lattice gas model with stochastic "diffusive" kinetics, the problems of rotation-translation corrections and "thermal nonaccommodation effects" do not arise;^(1,3,4) thus we can discuss the question of the extent to which the microscopic surface tension of a small cluster differs from the (macroscopic) surface tension of a flat, bulk surface, without the need to discuss these additional problems. We complement these simulation studies by low-temperature series expansions. In Section 5 we give our simulation results on the diffusivity of clusters, and tentatively interpret them in terms of several diffusion mechanisms. Section 6 contains our conclusions, and also an attempted speculative explanation of recent nucleation experiments.

2. THERMODYNAMICS OF CLUSTER-VAPOR EQUILIBRIUM

While the thermodynamics of cluster-vapor equilibrium has been studied extensively in the literature,⁽¹⁻⁴⁾ it is usual to consider equilibria either for constant chemical potential or in the thermodynamic limit. For our purposes it is essential, however, to consider the equilibrium at constant number of molecules $N < \infty$ in a finite volume V : As total density ρ we denote the ratio N/V : Since we are interested in the dependence of this equilibrium on the size of this volume, care has to be taken in not evoking thermodynamic relations which become valid only in the thermodynamic limit.

The situation may be understood by referring to Fig. 1, where the Helmholtz free energy F of the system is shown schematically as a function of cluster size l for three values of the chemical potential $\mu_1 < \mu_2 < \mu_3$. For each value of μ , F increases up to the critical cluster size and then decreases again. However, because of the constraint of a fixed total particle number N , μ and l are not independent, so that only the points indicated by solid dots are available to the system. The dash-dotted curve indicates the locus of such points; the thermodynamic equilibrium of the system is found at that point on the locus for which F is smallest. In this paper we locate this minimum by expansions about the coexistence line for which exact relations are known, exploiting the information on cluster properties which can be gained in this way. We start from the following relation for the grand potential Ω :

$$\Omega(T, V, \mu) = -\hat{p}V = F - \mu N \quad (1)$$

where T is the absolute temperature, and \hat{p} is a generalized pressure in a finite system,⁽³⁴⁾ which reduces to the ordinary pressure $p = -\partial\Omega/\partial V|_{\mu, T}$ for

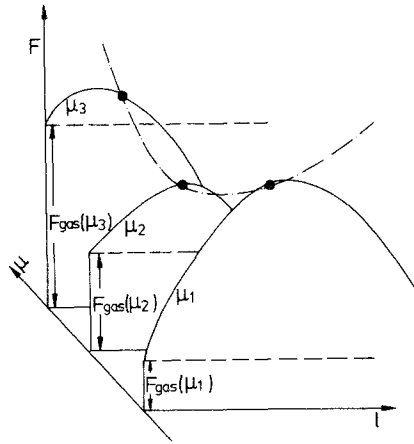


Fig. 1. Schematic plot of the free energy as a function of cluster size l and chemical potential μ . The curve shown as dashed-dotted indicates the states of the system with a fixed particle number N .

$V \rightarrow \infty$. We wish to expand Eq. (1) at chemical potential $\mu = \mu_c$ where bulk gas and liquid phases coexist. We denote the density at the coexistence curve by $\rho^{\text{coex}} = \rho(T, V, \mu = \mu_c)$, and expand the well-known identity $N = -(\partial\Omega/\partial\mu)_{T,V}$ to second order in $\mu - \mu_c$,

$$-(\partial\Omega/\partial\mu)_{T,V} = N = V\rho = V\rho^{\text{coex}} + V\chi(\mu - \mu_c) - \frac{1}{2}(\mu - \mu_c)^2 VC;$$

$$C \equiv \frac{1}{V} \left(\frac{\partial^3 \Omega}{\partial \mu^3} \right)_{T,V}, \quad \chi \equiv -\frac{1}{V} \left(\frac{\partial^2 \Omega}{\partial \mu^2} \right)_{T,V} \Big|_{\mu = \mu_c} \quad (2)$$

Similarly, introducing the grand potential per unit volume at the coexistence curve $\omega(\mu_c, T, V)$, we expand Eq. (1) to third order,

$$\Omega_{\text{gas}}(T, V, \mu) = V[\omega_{\text{gas}}(\mu_c, T, V) + (\mu_c - \mu)\rho_G^{\text{coex}} - \frac{1}{2}(\mu_c - \mu)^2 \chi_G - \frac{1}{6}(\mu_c - \mu)^3 C_G] \quad (3)$$

$$\Omega_{\text{liq}}(T, V, \mu) = V[\omega_{\text{liq}}(\mu_c, T, V) + (\mu_c - \mu)\rho_L^{\text{coex}} - \frac{1}{2}(\mu_c - \mu)^2 \chi_L - \frac{1}{6}(\mu_c - \mu)^3 C_L] \quad (4)$$

We now assume *periodic boundary conditions* for the volume V which contains the gas phase, and assumes temperatures T low enough such that the correlation length ξ of fluctuations is much smaller than the linear dimension $V^{1/d}$ of our d -dimensional box. Analyses of finite-size effects show then that⁽³⁵⁾ $\omega_{\text{gas}}(\mu_c, T, V) - \omega_{\text{gas}}(\mu_c, T, V \rightarrow \infty) \propto \exp(-V^{1/d}/\xi) \ll 1$, and similar relations hold for the size dependence of $\omega_{\text{liq}}(\mu_c, T, V)$, ρ_G^{coex} , ρ_L^{coex} , χ_G , χ_L , C_G , and C_L . Since we will be interested in finite-size corrections of order $1/V$, which are asymptotically much larger than any corrections of order $\exp(-V^{1/d}/\xi)$, we may neglect the volume dependence of all quantities within the square brackets in Eqs. (3) and (4).

We next consider a system of N molecules which consists of two subsystems, l molecules in a liquid cluster and $N - l$ molecules in the surrounding

gas, and neglect the interaction energy between the two subsystems. [This is rigorously correct in the lattice gas, where we may define a "cluster" to be a group of atoms linked together by nearest neighbor bonds. Then by definition no bonds cross the cluster surface. For a suitable definition of clusters in continuum systems see, e.g., Refs. 2, 22, and 30. In any case the following analysis is not affected by details of the cluster definition.] The volume V_l occupied by the cluster is approximately proportional to the number of molecules it contains, i.e.,

$$V_l = V_0(T, \mu)l \quad (5)$$

Since our subsystems are then additive, the condition that the total mass is conserved is expressed as

$$\begin{aligned} N &= l + [V - V_0(T, \mu)l]\rho_G(T, \mu) \\ &= l + \left[V - \frac{l}{\rho_L(T, \mu)} \right] \left[\rho_G^{\text{coex}} - (\mu_c - \mu)\chi_G - \frac{1}{2}(\mu_c - \mu)^2 C_G \right] \end{aligned} \quad (6)$$

Of course, the part of the system that we identify as "gas" contains physical clusters as well; even at the low temperatures considered in the simulations to be described in Section 4 the spontaneous formation of dimers, trimers, etc., was observed. But for typical conditions the total mass contained in the cluster exceeds that of the remaining gas; thus no second cluster in the considered range of sizes can form, and no problem of identifying the cluster arises.

Since

$$\begin{aligned} V_0(T, \mu) &= \frac{1}{\rho_L(T, \mu)} = \frac{1}{\rho_L^{\text{coex}} - (\mu_c - \mu)\chi_L - \frac{1}{2}(\mu_c - \mu)^2 C_L} \\ &\approx \frac{1}{\rho_L^{\text{coex}}} \left[1 + \frac{(\mu_c - \mu)\chi_L}{\rho_L^{\text{coex}}} + \frac{(\mu_c - \mu)^2}{\rho_L^{\text{coex}}} \left(\frac{C_L}{2} + \frac{\chi_L^2}{\rho_L^{\text{coex}}} \right) \right] \end{aligned} \quad (7)$$

Eq. (6) yields in leading order of $\rho - \rho_G^{\text{coex}}$

$$\begin{aligned} \mu - \mu_c &\approx \left[\rho - \rho_G^{\text{coex}} - \frac{l}{V} \left(1 - \frac{\rho_G^{\text{coex}}}{\rho_L^{\text{coex}}} \right) \right] \\ &\times \left\{ \chi_G \left[1 - \frac{l/V}{\rho_L^{\text{coex}}} \left(1 - \frac{\chi_L \rho_G^{\text{coex}}}{\chi_G \rho_L^{\text{coex}}} \right) \right] \right\}^{-1} \\ &\times \left\{ 1 + \frac{C_G}{2\chi_G^2} \left[\rho - \rho_G^{\text{coex}} - \frac{l}{V} \left(1 - \frac{\rho_G^{\text{coex}}}{\rho_L^{\text{coex}}} \right) \right] \right\} \\ &\times \left[1 - \frac{l/V}{\rho_L^{\text{coex}}} \left(1 - \frac{\chi_L \rho_G^{\text{coex}}}{\chi_G \rho_L^{\text{coex}}} \right) \right]^{-2} \end{aligned} \quad (8)$$

In the thermodynamic limit $V \rightarrow \infty$ this relation gives the standard result $\mu - \mu_c = (\rho - \rho_G^{\text{coex}})/\chi_G$, of course; for finite V it describes the reduction of chemical potential due to the formation of a liquid cluster. Equation (8) shows that for a given temperature, total density, and volume the size of the cluster l and the chemical potential μ are not independent variables but rather depend on each other.

From Eqs. (1) and (3) we obtain for the free energy of the gas phase in the system

$$F_{\text{gas}} = [V - V_0(T, \mu)l][\omega_{\text{gas}}(\mu_c, T) + (\mu_c - \mu)\rho_G^{\text{coex}} - \frac{1}{2}(\mu_c - \mu)^2\chi_G - \frac{1}{6}(\mu_c - \mu)^3C_G] + (N - l)\mu \tag{9}$$

$$F_l = F_l^{\text{surf}} + \mu l + \frac{V_0(T, \mu)l}{V} \Omega_{\text{liq}}(T, V, \mu) \tag{10}$$

Note that we do not make any specific assumption about the “surface correction” F_l^{surf} , and thus Eq. (10) should rather be considered as a definition of F_l^{surf} . Since the Helmholtz free energies of the two subsystems are additive (see also the discussion in Ref. 4), we have

$$F = F_{\text{gas}} + F_l = F_l^{\text{surf}} + N\mu + V(\mu_c - \mu)\rho_G^{\text{coex}} - \frac{1}{2}V\chi_G(\mu_c - \mu)^2 - \frac{1}{6}VC_G(\mu_c - \mu)^3 + V\omega_{\text{gas}}(\mu_c, T) + V_0(\mu, T)l[\omega_{\text{liq}}(\mu_c, T) - \omega_{\text{gas}}(\mu_c, T) + (\mu_c - \mu) \times (\rho_L^{\text{coex}} - \rho_G^{\text{coex}}) - \frac{1}{2}(\chi_L - \chi_G)(\mu_c - \mu)^2 - \frac{1}{6}(C_L - C_G)(\mu_c - \mu)^3] \tag{11}$$

Making use of the coexistence condition which defines $\mu_c(T)$,

$$\omega_{\text{liq}}(\mu_c, T) = \omega_{\text{gas}}(\mu_c, T)$$

we obtain from Eq. (11), using also Eq. (7),

$$F - N\mu_c - V\omega_{\text{gas}}(\mu_c, T) = F_l^{\text{surf}} + V\left\{(\mu - \mu_c)\left[\rho - \rho_G^{\text{coex}} - \frac{l}{V}\left(1 - \frac{\rho_G^{\text{coex}}}{\rho_L^{\text{coex}}}\right)\right] - \frac{1}{2}\chi_G(\mu - \mu_c)^2\left[1 - \frac{l/V}{\rho_L^{\text{coex}}}\left(1 - \frac{\rho_G^{\text{coex}}}{\rho_L^{\text{coex}}}\frac{\chi_L}{\chi_G}\right)\right] + \frac{1}{6}C_G(\mu - \mu_c)^3 \times \left\{1 - \frac{l/V}{\rho_L^{\text{coex}}}\left[1 + \frac{C_L}{C_G}\left(2 - 3\frac{\rho_G^{\text{coex}}}{\rho_L^{\text{coex}}}\right) + 3\frac{\chi_L^2}{C_G\rho_L^{\text{coex}}}\left(1 + \frac{\chi_G}{\chi_L} - 2\frac{\rho_G^{\text{coex}}}{\rho_L^{\text{coex}}}\right)\right]\right\}\right\} \tag{12}$$

Using Eq. (8), we find that this expression becomes further

$$\begin{aligned}
 F - N\mu_c - V\omega_{\text{gas}}(\mu_c, T) &= F_l^{\text{surf}} + \frac{V}{2\chi_G} \left[\rho - \rho_G^{\text{coex}} - \frac{l}{V} \left(1 - \frac{\rho_G^{\text{coex}}}{\rho_L^{\text{coex}}} \right) \right]^2 \\
 &\times \left[1 - \frac{l/V}{l_L^{\text{coex}}} \left(1 - \frac{\chi_L \rho_G^{\text{coex}}}{\chi_G \rho_L^{\text{coex}}} \right) \right]^{-1} \\
 &\times \left(1 + \frac{1}{3} \frac{C_G}{\chi_G^2} \left[\rho - \rho_G^{\text{coex}} - \frac{l}{V} \left(1 - \frac{\rho_G^{\text{coex}}}{\rho_L^{\text{coex}}} \right) \right] \right) \\
 &\times \left[1 - \frac{l/V}{\rho_L^{\text{coex}}} \left(1 - \frac{\chi_L \rho_G^{\text{coex}}}{\chi_G \rho_L^{\text{coex}}} \right) \right]^{-2} \\
 &\times \left\{ 1 - \frac{l/V}{\rho_L^{\text{coex}}} \left[1 + \frac{C_L}{C_G} \left(2 - 3 \frac{\rho_G^{\text{coex}}}{\rho_L^{\text{coex}}} \right) \right. \right. \\
 &\quad \left. \left. + 3 \frac{\chi_L^2}{C_G \rho_L^{\text{coex}}} \left(1 + \frac{\chi_G}{\chi_L} - 2 \frac{\rho_G^{\text{coex}}}{\rho_L^{\text{coex}}} \right) \right] \right\}
 \end{aligned} \tag{13}$$

We next expand Eq. (13) in powers of l/V as

$$\begin{aligned}
 F - N\mu_c - V\omega_{\text{gas}}(\mu_c, T) &= F_l^{\text{surf}} + \frac{V}{2\chi_G} (\rho - \rho_G^{\text{coex}})^2 \left(1 + \frac{C_G \rho_L^{\text{coex}}}{3\chi_G^2} \frac{\rho - \rho_G^{\text{coex}}}{\rho_L^{\text{coex}}} \right) - \frac{l}{\chi_G} (\rho - \rho_G^{\text{coex}}) \\
 &\times \left\{ \left(1 - \frac{\rho_G^{\text{coex}}}{\rho_L^{\text{coex}}} \right) - \frac{1}{2} \frac{\rho - \rho_G^{\text{coex}}}{\rho_L^{\text{coex}}} \left[\left(1 - \frac{\chi_L \rho_G^{\text{coex}}}{\chi_G \rho_L^{\text{coex}}} \right) - \frac{C_G \rho_L^{\text{coex}}}{\chi_G^2} \left(1 - \frac{\rho_G^{\text{coex}}}{\rho_L^{\text{coex}}} \right) \right] \right\} \\
 &+ \frac{l^2/V}{2\chi_G} \left(1 - \frac{\rho_G^{\text{coex}}}{\rho_L^{\text{coex}}} \right)^2 \left[1 + \frac{\rho - \rho_G^{\text{coex}}}{\rho_L^{\text{coex}}} \left(\frac{C_G \rho_L^{\text{coex}}}{\chi_G^2} - 2 \frac{1 - \chi_L \rho_G^{\text{coex}} / \chi_G \rho_L^{\text{coex}}}{1 - \rho_G^{\text{coex}} / \rho_L^{\text{coex}}} \right) \right] \\
 &+ \frac{l^3/V^2}{2\chi_G} \left(1 - \frac{\rho_G^{\text{coex}}}{\rho_L^{\text{coex}}} \right)^2 \frac{1}{\rho_L^{\text{coex}}} \left[\left(1 - \frac{\chi_L \rho_G^{\text{coex}}}{\chi_G \rho_L^{\text{coex}}} \right) - \frac{1}{3} \frac{C_G \rho_L^{\text{coex}}}{\chi_G^2} \left(1 - \frac{\rho_G^{\text{coex}}}{\rho_L^{\text{coex}}} \right) \right]
 \end{aligned} \tag{14}$$

Equation (14) can be considered as a systematic expansion simultaneously in the two small variables l/V and $\rho - \rho_G^{\text{coex}}$. Since we have kept only terms up to order $(\mu_c - \mu)^3$ in Eq. (11), we keep also only terms up to third order in our small variables in Eq. (14).

Since in thermal equilibrium at constant N , V , and T the free energy F must be a minimum, we require

$$\begin{aligned}
 0 &= \left(\frac{\partial F}{\partial l} \right)_{N,V,T} \\
 &= \left(\frac{\partial F_l^{\text{surf}}}{\partial l} \right)_T - \frac{(\rho - \rho_G^{\text{coex}})(1 - \rho_G^{\text{coex}}/\rho_L^{\text{coex}})}{\chi_G} \\
 &\quad \times \left\{ 1 + \frac{1}{2} \frac{\rho - \rho_G^{\text{coex}}}{\rho_L^{\text{coex}}} \left[\frac{C_G \rho_L^{\text{coex}}}{\chi_G^2} - \frac{1 - \chi_L \rho_G^{\text{coex}}/\chi_G \rho_L^{\text{coex}}}{1 - \rho_G^{\text{coex}}/\rho_L^{\text{coex}}} \right] \right\} \\
 &\quad + \frac{l/V}{\chi_G} \left(1 - \frac{\rho_G^{\text{coex}}}{\rho_L^{\text{coex}}} \right)^2 \left\{ 1 + \frac{\rho - \rho_G^{\text{coex}}}{\rho_L^{\text{coex}}} \left[\frac{C_G \rho_L^{\text{coex}}}{\chi_G^2} - 2 \frac{1 - \chi_L \rho_G^{\text{coex}}/\chi_G \rho_L^{\text{coex}}}{1 - \rho_G^{\text{coex}}/\rho_L^{\text{coex}}} \right] \right\} \\
 &\quad + \frac{(l/V)^2}{2\chi_G \rho_L^{\text{coex}}} \left(1 - \frac{\rho_G^{\text{coex}}}{\rho_L^{\text{coex}}} \right)^2 \left\{ 3 \left[\left(1 - \frac{\chi_L \rho_G^{\text{coex}}}{\chi_G \rho_L^{\text{coex}}} \right) - \frac{C_G \rho_L^{\text{coex}}}{\chi_G^2} \left(1 - \frac{\rho_G^{\text{coex}}}{\rho_L^{\text{coex}}} \right) \right] \right\}
 \end{aligned} \tag{15}$$

The solution of this equation yields the critical size l^* . The condition that F is a minimum and not a maximum at l^* is

$$\begin{aligned}
 0 &< \left(\frac{\partial^2 F}{\partial l^2} \right)_{N,V,T} \Big|_{l=l^*} \\
 &= \left(\frac{\partial^2 F_l^{\text{surf}}}{\partial l^2} \right)_T \Big|_{l=l^*} + \frac{(1 - \rho_G^{\text{coex}}/\rho_L^{\text{coex}})^2}{\chi_G V} \\
 &\quad \times \left\{ 1 + \frac{\rho - \rho_G^{\text{coex}}}{\rho_L^{\text{coex}}} \left[\frac{C_G \rho_L^{\text{coex}}}{\chi_G^2} - 2 \frac{1 - \chi_L \rho_G^{\text{coex}}/\chi_G \rho_L^{\text{coex}}}{1 - \rho_G^{\text{coex}}/\rho_L^{\text{coex}}} \right] \right\} \\
 &\quad + \frac{l^*/V^2}{\chi_G \rho_L^{\text{coex}}} \left(1 - \frac{\rho_G^{\text{coex}}}{\rho_L^{\text{coex}}} \right)^2 \\
 &\quad \times \left[3 \left(1 - \frac{\chi_L \rho_G^{\text{coex}}}{\chi_G \rho_L^{\text{coex}}} \right) - \frac{C_G \rho_L^{\text{coex}}}{\chi_G^2} \left(1 - \frac{\rho_G^{\text{coex}}}{\rho_L^{\text{coex}}} \right) \right]
 \end{aligned} \tag{16}$$

Since we have used an expansion which requires that $(\rho - \rho_G^{\text{coex}})/\rho_L^{\text{coex}} \ll 1$, the second term on the right-hand side is always positive (we need not be concerned with the third term here, since it is smaller by a factor of l^*/V than the second one). However, since this term is proportional to the inverse of the volume, it can outweigh the negative term $(\partial^2 F_l^{\text{surf}}/\partial l^2)_T$ only if V is not too large. As noted above, the equilibrium between a finite cluster and surrounding (supersaturated) gas is always unstable in the thermodynamic limit.

Before we apply Eq. (15) we have to check if the equilibrium described by this equation is actually stable or only metastable. For that purpose we have to compare the free energy, as given by Eq. (14) with $l = l^*$, with the

free energy of a supersaturated gas without a cluster, assuming the same values of N , V , and T . Using Eq. (3), we find

$$F_{\text{gas}} - N\mu_c - V\omega_{\text{gas}}(\mu_c, T) = V[(\mu - \mu_c)(\rho - \rho_G^{\text{coex}}) - \frac{1}{2}\chi_G(\mu - \mu_c)^2 + \frac{1}{6}C_G(\mu - \mu_c)^3] \quad (17)$$

and, using Eq. (2),

$$F_{\text{gas}} - N\mu_c - V\omega_{\text{gas}}(\mu_c, T) = V\left[\frac{(\rho - \rho_G^{\text{coex}})^2}{2\chi_G} + \frac{C_G}{6\chi_G^3}(\rho - \rho_G^{\text{coex}})^3\right] \quad (18)$$

From Eqs. (14) and (18) we conclude, keeping now quadratic terms in our small variables l/V and $\rho - \rho_G^{\text{coex}}$ only and treating for simplicity the case of low temperatures where $\rho_G^{\text{coex}} \ll \rho_L^{\text{coex}}$, that

$$\Delta F \equiv F - F_{\text{gas}} \approx F_l^{\text{surf}} - \frac{l^*}{\chi_G}(\rho - \rho_G^{\text{coex}}) \quad (19)$$

while Eq. (16) simplifies with the same approximations to

$$\left(\frac{\partial^2 F}{\partial l^2}\right)_{N,V,T}|_{l=l^*} = \left(\frac{\partial^2 F_l^{\text{surf}}}{\partial l^2}\right)_T|_{l=l^*} + \frac{1}{V\chi_G} \quad (20)$$

In the same approximation Eq. (16) simplifies to

$$\left(\frac{\partial F_l^{\text{surf}}}{\partial l}\right)_T = \frac{\rho - \rho_G^{\text{coex}} - l/V}{\chi_G} \quad (21)$$

so that the equilibrium is stable if

$$\Delta F < 0 \quad (22)$$

We discuss Eq. (22) only for the example where one approximates F_l^{surf} by the ‘‘capillarity approximation,’’ i.e.,

$$F_l^{\text{surf}} = S_d f_s(T) (l/V_d \rho_L^{\text{coex}})^{1-1/d} \quad (23)$$

where S_d and V_d are the surface and volume of a d -dimensional unit sphere, and $f_s(T)$ is an effective surface tension. From Eqs. (21) and (23) it is easy to find that

$$\left(1 - \frac{1}{d}\right) S_d \frac{f_s(T)}{(V_d \rho_L^{\text{coex}})^{1-1/d}} \chi_G + (l^*)^{1/d} \frac{l^*}{V} = (l^*)^{1/d} (\rho - \rho_G^{\text{coex}}) \quad (24)$$

Since Eqs. (23), (22), and (19) lead to

$$S_d \frac{f_s(T)}{(V_d \rho_L^{\text{coex}})^{1-1/d}} \chi_G < (l^*)^{1/d} (\rho - \rho_G^{\text{coex}}) \quad (25)$$

we can use Eq. (24) to find the condition of stability

$$\frac{1}{d} S_d \frac{f_s(T)}{(V_d \rho_L^{\text{coex}})^{1-1/d}} < (l^*)^{1/d} \frac{l^*}{V} \quad (26)$$

On the other hand, the condition for at least metastability, $(\partial^2 F/\partial l^2)_{N,V,T} > 0$, yields, with the help of Eqs. (20) and (23), the somewhat weaker condition

$$\frac{1}{d} \left(1 - \frac{1}{d}\right) S_d \frac{f_s(T)}{(V_d \rho_L^{\text{coex}})^{1-1/d}} < (l^*)^{1/d} \frac{l^*}{V} \quad (27)$$

Both Eqs. (27) and (26) show once more that other than unstable equilibria are possible for finite values of l/V only. The condition for metastability is weaker than the condition for stability by only a factor $1 - 1/d$. Of course, this particular result relies on the very special assumption made in Eq. (23). However, the treatment is immediately generalized to the case where d in Eq. (20) is treated as an “effective dimensionality” of the clusters for the values of l under consideration, and $f_s(T)$ is then the appropriate “microscopic surface tension.”

In order to interpret the physical meaning of the equilibrium condition, Eq. (15), it is convenient to introduce the density ρ_G of the gas surrounding the cluster, i.e.,

$$\rho_G \equiv (N - l^*)/V_G, \quad V_G = V - V_0(T, \mu)l^* = V - l^*/\rho_L(T, \mu) \quad (28)$$

From Eqs. (7), (28), and (8) it is easy to find the following expansion, keeping terms up to second order in the small quantities $\rho_G, \rho_G^{\text{coex}}, l/V$ only:

$$\rho - \rho_G^{\text{coex}} = (\rho_G - \rho_G^{\text{coex}}) + \frac{l^*}{V} - \frac{l^*/V}{\rho_L^{\text{coex}}} \rho_G \quad (29)$$

Inserting this expression into Eq. (15), we obtain by a straightforward calculation

$$\begin{aligned} \chi_G \left(\frac{\partial F_l^{\text{surf}}}{\partial l} \right)_{T, l^*} / (\rho_L^{\text{coex}} - \rho_G^{\text{coex}}) &= \frac{\rho_G - \rho_G^{\text{coex}}}{\rho_L^{\text{coex}}} \\ &\times \left[\left(1 + \frac{1}{2} \frac{\rho_G - \rho_G^{\text{coex}}}{\rho_L^{\text{coex}}} \left(\frac{C_G \rho_L^{\text{coex}}}{\chi_G^2} - 1 \right) \right) \right] \end{aligned} \quad (30)$$

In Eq. (30) all terms of higher than second order in the small variables $\rho_G, \rho_G^{\text{coex}}$, and l/V have been omitted on the right-hand side. This neglect is legitimate since in Eq. (13) we have kept up to third-order terms, and by taking the derivative in Eq. (15) the highest order of terms taken into account consistently was reduced by one. Note that in contrast to what one expects from Eq. (15) at first sight, there are no l^*/V corrections in Eq. (30).

Since at low temperatures $\rho_G - \rho_G^{\text{coex}} \ll \rho_L^{\text{coex}}$ one might expect that the correction in square brackets in Eq. (30) is negligible. However, this is not so: since $-C_G/\chi_G^2 \approx 1/\rho_G^{\text{coex}}$ (in the ideal gas case this result would be precisely correct), the correction in square brackets is of order $(\rho_G - \rho_G^{\text{coex}})/\rho_G^{\text{coex}}$, which

need not be negligibly small. In order to elucidate this term, we use Eq. (29) in Eq. (8) to find

$$\mu - \mu_c \approx \frac{\rho_G - \rho_G^{\text{coex}}}{\chi_G} \left[1 + \frac{C_G}{2\chi_G^2} (\rho_G - \rho_G^{\text{coex}}) \right] \quad (31)$$

where again all terms higher than second order in the small quantities ρ_G , ρ_G^{coex} , and l/V have been omitted on the right-hand side. Hence Eq. (30) can be rewritten as

$$\left(\frac{\partial F_l^{\text{surf}}}{\partial l} \right)_T \Big|_{l^*} = (\mu - \mu_c) \left(1 - \frac{\rho_G^{\text{coex}}}{\rho_L^{\text{coex}}} \right) \quad (32)$$

which is nothing else but the well-known "Kelvin equation."⁽¹⁾ Note that the difference in bulk Gibbs potential between the liquid cluster and the surrounding gas is $l(\mu - \mu_c)(1 - \rho_G^{\text{coex}}/\rho_L^{\text{coex}})$: The bulk Gibbs potential of the liquid droplet is $(\mu - \mu_c)l$, the Gibbs potential of the gas taking the same volume is $(\mu - \mu_c)l\rho_G^{\text{coex}}/\rho_L^{\text{coex}}$. This correction factor $1 - \rho_G^{\text{coex}}/\rho_L^{\text{coex}}$ often is neglected but becomes important if one treats nucleation close to the critical point.

Finally we draw attention to a consequence of the fact that l and μ depend on each other via Eq. (8), and hence a further correction in Eq. (15) may arise due to an explicit dependence of F_l^{surf} on the chemical potential μ . In fact, we have

$$\left(\frac{\partial F_l^{\text{surf}}}{\partial l} \right)_T = \left(\frac{\partial F_l^{\text{surf}}}{\partial l} \right)_{T,\mu} + \left(\frac{\partial F_l^{\text{surf}}}{\partial \mu} \right)_{T,l} \frac{d\mu}{dl} \quad (33)$$

and using Eq. (8) this becomes in leading order

$$\left(\frac{\partial F_l^{\text{surf}}}{\partial l} \right)_T = \left(\frac{\partial F_l^{\text{surf}}}{\partial l} \right)_{T,\mu} \left\{ 1 - \left[\left(\frac{\partial F_l^{\text{surf}}}{\partial \mu} \right)_{T,l} / \left(\frac{\partial F_l^{\text{surf}}}{\partial l} \right)_{T,\mu} \right] \frac{1 - \rho_G^{\text{coex}}/\rho_L^{\text{coex}}}{\chi_G V} \right\} \quad (34)$$

Since the ratio of derivatives $(\partial F_l^{\text{surf}}/\partial \mu)_{T,l}/(\partial F_l^{\text{surf}}/\partial l)_{T,\mu}$ is of order l , we immediately realize that the correction on the right-hand side of Eq. (34) is of order l/V and hence small. Thus it is legitimate to estimate it by means of the capillarity approximation, Eq. (23), where we now include a dependence of the surface tension $f_s(T, \mu)$ on the chemical potential μ . Then Eq. (34) can be rewritten more explicitly as

$$\left(\frac{\partial F_l^{\text{surf}}}{\partial l} \right)_T = \left(\frac{\partial F_l^{\text{surf}}}{\partial l} \right)_{T,\mu} \left\{ 1 - \left[\frac{\partial}{\partial \mu} \ln f_s(T, \mu) \right]_T \frac{1 - \rho_G^{\text{coex}}/\rho_L^{\text{coex}}}{\chi_G(1 - 1/d)} \frac{l}{V} \right\} \quad (35)$$

In the Appendix it is shown that in the lattice gas at low temperatures $f_s(T, \mu)$ is quadratic in $(\mu - \mu_c)$, i.e.,

$$f_s(T, \mu) = f_s(T, \mu_c) + \frac{1}{2}\chi_s(\mu - \mu_c)^2 \quad (36)$$

and where the leading term in the low-temperature expansion of χ_s is estimated. Since by our expansion in powers of $(\mu - \mu_c)$ in Eqs. (3), (4), and (12) we are restricted to the case where $(\mu - \mu_c)$ is a small variable, the correction factor in Eq. (35) is of order $(\mu - \mu_c)l/V$ and hence of *second* order in our small variables. Since the right-hand sides of Eqs. (30) and (32) are of first order in the small variables, use of Eqs. (35) and (36) would produce a term of third order only, which can be omitted, since other third-order terms have been neglected as well.

We emphasize that while our treatment leading up to Eq. (23) is completely general, the absence of a linear term in Eq. (36) may occur only in the lattice gas model due to its special symmetry properties (Appendix), and hence the correction in Eqs. (34) and (35) may be more important for other systems. In principle, Eqs. (32) and (34) allow a separate determination of both derivatives $(\partial F_i^{\text{surf}}/\partial l)_{T,\mu}$ and $(\partial F_i^{\text{surf}}/\partial \mu)_{T,l}$ by studying the equilibrium for the same value of l^* in a range of values for V : the chemical potential difference $\mu^* - \mu_c$ at which equilibrium is established should then have a linear variation with the variable l^*/V . Then $(\partial F_i^{\text{surf}}/\partial l)_{T,\mu}$ follows from an extrapolation of this linear variation of μ^* to $l^*/V = 0$, while $(\partial F_i^{\text{surf}}/\partial \mu)_{T,\mu}$ follows from the slope of $d\mu^*/d(l^*/V)$, as Eq. (35) shows. In practice, however, this procedure can be prohibitively difficult due to statistical inaccuracies in the numerical determination of μ^* and l^* .

3. ESTIMATES FOR THE CLUSTER FREE ENERGY IN THE CLUSTER DEFINITION DUE TO ABRAHAM AND REISS ET AL.

Reiss *et al.*⁽²⁷⁾ and Abraham *et al.*^(4,28) suggested that one might study a cluster by constructing a constraining sphere around its center of gravity; all N molecules within the sphere are counted as part of the cluster. In order to allow for fluctuations in cluster shape (and thus include configurational entropy contributions to the cluster free energy), it is necessary to make the volume V of this sphere distinctly larger than the volume V_l defined in Eq. (5). While studies were made in the range from $V \approx 2V_l$ to $V \approx 10^3 V_l$, it was suggested that the cluster free energy might be estimated by using V of the order of $10V_l$. We examine this prescription within the context of our treatment, comparing the free energy of our system of $N - l^*$ gas atoms and the cluster with l^* atoms with the free energy of a cluster with N atoms.

From Eqs. (4) and (10) we have for a cluster of N atoms, by definition,

$$F_N = F_N^{\text{surf}} + \mu N + V_0(T, \mu)N[\omega_{\text{liq}}(\mu_c, T, V) + (\mu_c - \mu)\rho_L^{\text{coex}} - \frac{1}{2}(\mu_c - \mu)^2\chi_L] \quad (37)$$

Using Eq. (7), we can rewrite this as follows, keeping terms up to order $(\mu - \mu_c)^2$ only,

$$\begin{aligned}
 F_N = F_N^{\text{surf}} + \mu N + V \frac{\rho}{\rho_L^{\text{coex}}} & \left\{ \omega_{\text{gas}}(\mu_c, T) - (\mu - \mu_c) \right. \\
 & \times \left| \rho_L^{\text{coex}} + \frac{\chi_L}{\rho_L^{\text{coex}}} \omega_{\text{gas}}(\mu_c, T) \right| \\
 & \left. + \frac{1}{2} (\mu - \mu_c)^2 \left[\chi_L + \frac{\omega_{\text{gas}}(\mu_c, T)}{\rho_L^{\text{coex}}} \left(C_L + \frac{2\chi_L^2}{\rho_L^{\text{coex}}} \right) \right] \right\}
 \end{aligned} \tag{38}$$

On the other hand we may combine Eqs. (13), (29), and (31) to obtain

$$\begin{aligned}
 F & \approx F_{i^*}^{\text{surf}} + N\mu_c + V\omega_{\text{gas}}(\mu_c, T) + \frac{V}{2\chi_G} (\rho_G - \rho_G^{\text{coex}})^2 \left(1 - \frac{l^*/V}{\rho_L^{\text{coex}}} \right) \\
 & \times \left[1 + \frac{1}{3} \frac{C_G}{\chi_G^2} (\rho_G - \rho_G^{\text{coex}}) \right] \left(1 - \frac{l^*/V}{\rho_L^{\text{coex}}} \right) \\
 & \approx F_{i^*}^{\text{surf}} + N\mu_c + V\omega_{\text{gas}}(\mu_c, T) + \frac{V}{2} \chi_G (\mu - \mu_c)^2
 \end{aligned} \tag{39}$$

where Eq. (32) can be used to express $\mu - \mu_c$ in terms of $(\partial F_i^{\text{surf}}/\partial l)_T|_{i^*}$. From Eqs. (38) and (39) it is easy to find that

$$\begin{aligned}
 F_N - F = F_N^{\text{surf}} - F_{i^*}^{\text{surf}} - V\omega_{\text{gas}}(\mu_c, T) & \left[1 - \frac{\rho}{\rho_L^{\text{coex}}} \left(1 - \frac{\chi_L(\mu - \mu_c)}{\rho_L^{\text{coex}}} \right) \right] \\
 - \frac{V}{2} \chi_G (\mu - \mu_c)^2 & \left\{ 1 - \frac{\rho}{\rho_L^{\text{coex}}} \left[\frac{\chi_L}{\chi_G} + \frac{\omega_{\text{gas}}(\mu_c, T)}{\rho_L^{\text{coex}} \chi_G} \left(C_L + \frac{2\chi_L^2}{\rho_L^{\text{coex}}} \right) \right] \right\}
 \end{aligned} \tag{40}$$

We want to find out how well F_N is approximated by F ; i.e., we ask how small is the ratio $(F - F_N)/F_N^{\text{surf}}$, to estimate the relative error of F_N^{surf} . Since we are interested in the case where $l^* \gg 1$ only and low temperatures, where the gas density is very small, we have $N - l^* \ll l^*$: most of the molecules within the constraining sphere are contained in the cluster, and only a few in the surrounding gas. Hence we may expand F_N^{surf} , using once more Eq. (29),

$$F_N^{\text{surf}} = F_{i^*}^{\text{surf}} + \frac{\partial F_{i^*}^{\text{surf}}}{\partial l} \Big|_{i^*} (N - l^*) \approx F_{i^*}^{\text{surf}} + \frac{\partial F_{i^*}^{\text{surf}}}{\partial l} \Big|_{i^*} V\rho_G \left(1 - \frac{l^*/V}{\rho_L^{\text{coex}}} \right) \tag{41}$$

From Eqs. (32), (40), and (41) we hence obtain

$$\begin{aligned} \frac{F_N - F}{V} = & -\omega_{\text{gas}}(\mu_c, T) \left[1 - \frac{\rho}{\rho_L^{\text{coex}}} \left(1 - \frac{\chi_L(\mu - \mu_c)}{\rho_L^{\text{coex}}} \right) \right] \\ & + (\mu - \mu_c) \rho_G \left(1 - \frac{\rho_G^{\text{coex}}}{\rho_L^{\text{coex}}} \right) \left(1 - \frac{l^*/V}{\rho_L^{\text{coex}}} \right) - \frac{1}{2} \chi_G (\mu - \mu_c)^2 \\ & \times \left\{ 1 - \frac{\rho}{\rho_L^{\text{coex}}} \left[\frac{\chi_L}{\chi_G} + \frac{\omega_{\text{gas}}(\mu_c, T)}{\rho_L^{\text{coex}} \chi_G} \left(C_L + \frac{2\chi_L^2}{\rho_L^{\text{coex}}} \right) \right] \right\} \end{aligned} \quad (42)$$

We note that because of $\rho_G = \rho_G^{\text{coex}} + \chi_G(\mu - \mu_c) + \dots$ the negative third term on the right-hand side of Eq. (42) yields a small correction to the positive second term only. Note that $\omega_{\text{gas}}(\mu_c, T) < 0$, of course.

In the low-temperature regime where the cluster definition due to Reiss *et al.*⁽²⁷⁾ and Abraham *et al.*⁽²⁸⁾ is useful, we obtain from Eq. (42) a numerical estimate for this ratio $(F_N - F)/F_N^{\text{surf}}$ accurate to at least about $\pm 50\%$ by treating the gas phase at the coexistence curve as an ideal gas, and using the capillarity approximation in Eq. (32). Since for $V = 10V_*$, both factors $\rho/\rho_L^{\text{coex}}$ and $(l^*/V)/\rho_L^{\text{coex}}$ yield corrections of order 10^{-1} only, we approximate Eq. (42) as follows:

$$\begin{aligned} (F_N - F)/V \approx & \omega_{\text{gas}}(\mu_c, T) + (\mu - \mu_c) \rho_G - \frac{1}{2} \chi_G (\mu - \mu_c)^2 \\ = & \rho_G^{\text{coex}} k_B T + (\mu - \mu_c) \rho_G - \frac{1}{2} (k_B T)^{-1} \rho_G^{\text{coex}} (\mu - \mu_c)^2 \end{aligned} \quad (43)$$

and hence we find, since Eqs. (23) and (32) yield $F_i^{\text{surf}} = l^*(\mu - \mu_c)/(1 - 1/d) \approx N(\mu - \mu_c)/(1 - 1/d)$,

$$\frac{F_N - F}{F_N^{\text{surf}}} \approx \frac{F_N - F}{F_i^{\text{surf}}} = \left(1 - \frac{1}{d} \right) \frac{1}{\rho} \left[\rho_G^{\text{coex}} / \left(\frac{\mu - \mu_c}{k_B T} \right) + \rho_G - \frac{1}{2} \rho_G^{\text{coex}} \frac{\mu - \mu_c}{k_B T} \right] \quad (44)$$

For small $(\mu - \mu_c)k_B T$ it is seen that the relative difference $(F_N - F)/F_N^{\text{surf}}$ is of the order of $(\rho_G^{\text{coex}}/\rho)/[(\mu - \mu_c)/k_B T]$. Since $(\mu - \mu_c)/k_B T \rightarrow 0$ as $N \rightarrow \infty$, this difference becomes appreciable even if $\rho_G^{\text{coex}}/\rho$ is very small. This result is obvious from Eq. (43) already, of course, since $F_N - F \propto V \propto N$, while $F_N^{\text{surf}} \propto N^{1-1/d}$ only: thus the ratio in Eq. (44) must become large for large enough N . Thus this cluster definition becomes very inaccurate even for low temperatures, if the clusters are very large. However, in many cases of interest N is not so large and hence $(\mu - \mu_c)/k_B T$ is not small. Then the difference $(F_N - F)/F_N^{\text{surf}}$ may be quite small, and a meaningful estimation of F_N^{surf} from this definition becomes possible. In fact, for the “12-6 Lennard-Jones argon liquid” which has been studied^(4,27) the parameters to be used in Eq. (23), i.e., $F_N^{\text{surf}} = 4\pi f_s(T)(3N/4\pi\rho_L^{\text{coex}})^{2/3}$,³ are for $T = 84 \text{ K}$,⁽⁴⁾ $f_s(T) = 16.18 \text{ dyn/cm}$,

³ Note that a factor 4π is missing in the corresponding expression of Eq. (9.5.5) on p. 216 of Ref. 4.

$\rho_L^{\text{coex}} = 2.05 \times 10^{22}/\text{cm}^3$. Thus from Eq. (32), i.e., $(\mu - \mu_c)/k_B T = (2/3)F_N^{\text{surf}}/(Nk_B T)$, one readily obtains for $N = 100$, the largest size studied, that $(\mu - \mu_c)/k_B T \approx 1.29$. Since in the ideal gas case we have $\rho_G = \rho_G^{\text{coex}} \exp[(\mu - \mu_c)/k_B T]$, Eq. (44) becomes

$$\frac{F_N - F}{F_N^{\text{surf}}} \approx \frac{2}{3} \frac{\rho_G^{\text{coex}}}{\rho} \left(\frac{k_B T}{\mu - \mu_c} + \exp \frac{\mu - \mu_c}{k_B T} - \frac{1}{2} \frac{\mu - \mu_c}{k_B T} \right) \approx 2.51 \frac{\rho_G^{\text{coex}}}{\rho}$$

From the gas pressure at the coexistence curve, $p_G^{\text{coex}} = 595.35 \text{ Torr}$,⁽⁴⁾ we estimate $\rho_G^{\text{coex}} = p^{\text{coex}}/(k_B T) = 6.90 \times 10^{19}/\text{cm}^3$. Since $\rho = \rho_L^{\text{coex}}/10 = 2.05 \times 10^{21}/\text{cm}^3$, we get $(F_N - F)/F_N^{\text{surf}} \approx 0.85 \times 10^{-1}$. Thus one would get an unreliable estimate for F_N^{surf} if one approximated F_N by F in that case as done in Refs. 4 and 28, as expected in Ref. 30. For the smallest size studied ($N = 13$) the same estimate yields $(F_N - F)/F_N^{\text{surf}} \approx 2.4 \times 10^{-1}$. Clearly, due to the approximations made, these estimates are order-of-magnitude estimates only. But note that one obtains a similar conclusion using the pressure that was actually obtained from the simulation, which was (Ref. 4, Fig. 9.2) $p \approx 4 \times 10^5 \text{ dyn/cm}^2 \approx 300 \text{ Torr}$ for $V \approx 10V_l$, implying $\rho_G \approx 3.5 \times 10^{19}/\text{cm}^3$, $\rho_G^{\text{coex}} \approx 0.96 \times 10^{19}/\text{cm}^3$: This density is nearly an order of magnitude smaller, and the resulting errors in F_N^{surf} would be a few percent only. Presumably the former estimate is more realistic, since from the radial density profiles observed^(4,27) one notes that $\rho_G/\rho_L^{\text{coex}} \approx 10^{-2}$ close to the surface of the constraining box, while from $\rho_G^{\text{coex}} = 6.9 \times 10^{19}/\text{cm}^3$ we get $\rho_G/\rho_L^{\text{coex}} = \rho_L^{\text{coex}} \exp[(\mu - \mu_c)/k_B T] \approx 1.25 \times 10^{-2}$. Finally we note that from $\mu_c = -1.5685 \times 10^{-13} \text{ erg}$ we get $\rho_G^{\text{coex}} = [(2\pi mk_B T)^{3/2}/h]^3 \exp(\mu_c/k_B T) = 5 \times 10^{19}/\text{cm}^3$. From these considerations we obtain two general conclusions: (i) the cluster definition due to Reiss *et al.* and Abraham produces an error of about 10% in F_N^{surf} for gas densities exceeding $\rho_G^{\text{coex}}/\rho_L^{\text{coex}} \approx 10^{-3}$, while for low enough gas densities it clearly is accurate and very convenient; (ii) for the choice $V \leq 10V_l$ the gas density at the surface of the box may still be a bit larger than the equilibrium value ρ_G , i.e., one cuts off the outer parts of the interface profile between cluster and surrounding gas, as the above comparison of the observed density at the surface of the box⁽⁴⁾ and the outer estimates for ρ_G show.

Finally we consider the pV diagram of the system consisting of the cluster and the surrounding gas. From Eqs. (1) and (39) we conclude $[\omega_{\text{gas}}(\mu_c, T) = -p_G^{\text{coex}}]$

$$\begin{aligned} \hat{p} &= p_G^{\text{coex}} + \frac{N(\mu - \mu_c) - F_l^{\text{surf}}}{V} - \frac{1}{2} \chi_G (\mu - \mu_c)^2 \\ &\approx p_G^{\text{coex}} + \frac{(\mu - \mu_c)[N - l^*/(1 - 1/d)]}{V} - \frac{\chi_G}{2} (\mu - \mu_c)^2 \end{aligned} \quad (45)$$

For small V all molecules are part of the liquid phase. The pressure is then very large and decreases with increasing volume [this regime is of course not

described by Eq. (45), which holds for $(l^*/V)/\rho_L^{\text{coex}} \ll 1$]. When the pressure has decreased down to p_G^{coex} , the two-phase regime starts. Since the gas phase is supersaturated, we have $\mu > \mu_c$; but since at low temperatures for not too small $(l^*/V)/\rho_L^{\text{coex}}$ still most of the molecules are part of the liquid cluster, $N - l^* \ll l^*$ and hence the factor $N - l^*/(1 - 1/d) < 0$: thus the second term on the right-hand side of Eq. (45) is negative, and for small enough p_G^{coex} also $\hat{p} < 0$. Since l^* decreases with increasing V , the second term on the right-hand side of Eq. (45) changes sign for some large enough V , and so does \hat{p} . In between one then has a minimum $\hat{p}_{\text{min}} < 0$. On the other hand, for very large V all molecules of the system are in the gas phase; the pressure then is positive and decreases with V as $k_B T N/V$. Hence, in between, the pressure has a maximum $\hat{p}_{\text{max}} > 0$. Since Eq. (45) is rewritten with the help of Eq. (29) as

$$\begin{aligned} \hat{p} &= p_G^{\text{coex}} + \rho_G^{\text{coex}}(\mu - \mu_c) + \frac{\chi_G}{2}(\mu - \mu_c)^2 - \frac{l^*}{V}(\mu - \mu_c)\left(\frac{\rho_G}{\rho_L^{\text{coex}}} - \frac{1}{d-1}\right) \\ &= p_G - \frac{l^*}{V}(\mu - \mu_c)\left(\frac{\rho_G}{\rho_L^{\text{coex}}} - \frac{1}{d-1}\right) \end{aligned} \tag{46}$$

we note that it is a reasonable approximation to identify p_G with \hat{p} in the regime where $(l^*/V)/\rho_L^{\text{coex}} \ll 1$, $(\mu - \mu_c)/k_B T \ll 1$.

4. MONTE CARLO SIMULATION OF “CRITICAL CLUSTERS” IN THE TWO-DIMENSIONAL LATTICE GAS

The two-dimensional lattice gas (square lattice) is not a realistic model for any physical system, except perhaps for the study of adsorption on surfaces, assuming that the adatoms may only occupy “preferred sites” forming a square lattice.^(32,36) Even then the assumption that one has only nearest neighbor attractive interaction between adatoms apart from the binding forces to the substrate will be an oversimplification. The same is true for the approximation where crystal growth is described in terms of a Kossel model (see Ref. 37 for a review), and where at low temperatures and small values of the chemical potential difference one makes the further assumption that the $(n + 1)$ th layer starts forming only after the n th layer has been fully completed.⁽³⁷⁾ However, for our purposes, the model has many advantages (cf. also Ref. 38):

- (i) Due to the absence of any inertial motion in the lattice gas model, the problem of rotation–translation corrections does not arise, and thus we can concentrate on the question of the extent to which the “microscopic surface tension” of a small cluster differs from the macroscopic surface

tension $f_s(T, \mu)$ of a flat surface between bulk phases. Fortunately both μ_c and $f_s(T, \mu_c)$ are known rigorously from Onsager's exact solution.⁽³³⁾

(ii) Other quantities entering our expressions, like ρ_G^{coex} , ρ_L^{coex} , χ_G , χ_L , etc., are either also known rigorously⁽³⁸⁾ or with high numerical precision from low-temperature series expansions.⁽⁴⁰⁾ For details of the transcription⁽⁴¹⁾ from the "language" appropriate to an Ising ferromagnet^(38,39) to the lattice gas "language" see the Appendix.

(iii) For very small cluster sizes ($l = 1, 2, \dots, 6$), where the quasi-macroscopic treatment of Section 2 does not apply, one can easily estimate the cluster free energies F_l quite reliably from low-temperature series expansions (see also the Appendix).

(iv) Since the dynamics of the lattice gas model is described in terms of a Markovian master equation appropriate for stochastic evaporation and condensation of atoms,^(38,42) it is correct to treat the equilibrium between cluster and surrounding gas as strictly isothermal, the "thermal nonaccommodation problem"^(1,14) does not arise, and a meaningful comparison with classical nucleation theory is possible.

(v) The computer simulation by means of Monte Carlo methods⁽⁴⁵⁾ can be very efficiently applied to this problem.

(vi) Albeit unrealistic, the lattice gas is much more realistic than percolation models,⁽⁴⁴⁾ where clusters form via random mixing, and hence the interplay between entropy and energy is not at all described.

The computer simulations are done as follows: As initial condition, a fully compact cluster with l_i occupied sites is generated and put in the center of an $L \times L$ square lattice. Usually this initial cluster is chosen to have circular shape. Then N_i "gas" sites are randomly chosen to be occupied. This initial condition then defines the density $\rho = (l_i + N_i)/L^2$ for the particular run. The Monte Carlo run is performed utilizing the Kawasaki nearest neighbor exchange mechanism,⁽⁴²⁾ which was previously used for studies of the phase separation kinetics⁽⁴⁵⁻⁴⁷⁾ and is described there in detail. In most runs the temperature was $2J/k_B T = 1.5$ (i.e., $T/T_c \approx 0.59$), where J is the nearest neighbor interaction energy. A few runs with $2J/k_B T = 2$ (i.e., $T/T_c \approx 0.44$) were also performed. The surfaces of the box are connected by periodic boundary conditions to avoid surface effects: i.e., an atom diffusing out of the box at one side enters again on the opposite side of the box. Since the exchange $\rho_i \rightarrow \rho_j$, $\rho_j \rightarrow \rho_i$ ($\rho_i = 0, 1$ is the local density at lattice site i ; see the Appendix) conserves the total density, the analysis of Section 2 is applicable. One then lets the system develop until the equilibrium described there is reached: if the initial gas density $\rho_G^i = N_i/(L^2 - l_i)$ is higher than the ρ_G that characterizes the equilibrium, gas atoms have to condense at the cluster and hence $l^* > l_i$, while for $\rho_G^i < \rho_G$ atoms have to evaporate from the cluster in order to establish equilibrium, and $l^* < l_i$.

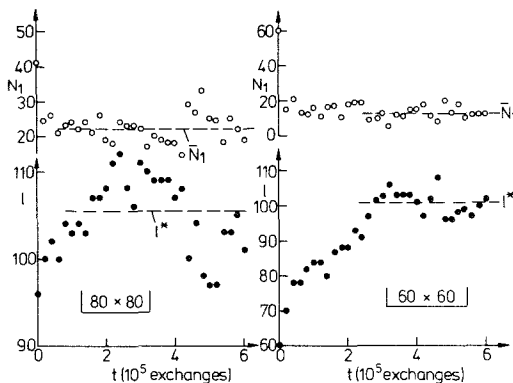


Fig. 2. Size of cluster l and number of monomers plotted vs time for the initial conditions $N_{1i} = 41, l_i = 96$ (left part) and $N_{1i} = 60, l_i = 60$ (right part). Dashed lines indicate the estimates for the thermal equilibrium.

Typically, runs with 600,000 exchanges were made, the first 150,000 of which were discarded, since equilibrium was not yet reached. Figure 2 gives two typical examples of time evolutions. The large fluctuations around l^* are expected from Eqs. (16) and (20), which show that the minimum of F at $l = l^*$ is very flat. The large time constant over which these fluctuations are correlated can be understood by recent theories on cluster dynamics^(4B): the relaxation time increases very strongly with cluster size. The strong decrease of the number N_1 of monomers at the beginning of the simulation is due to the formation of dimers, trimers, etc., in the gas phase. If the initial state is too far away from equilibrium, clusters of intermediate size are formed in the gas phase, which are incorporated into the main large cluster at a very slow rate only (see right part of Fig. 2, where l^* reaches the equilibrium much slower than N_1). In such cases it may happen that some “drift” of the “equilibrium” is observed throughout the run, which then has to be wholly discarded. Hence it is important to choose the initial state not too far from the expected final state, to avoid these slow relaxation effects.

Clearly, simple runs as shown in Fig. 2 do not yield accurate estimates of \bar{l} and \bar{N}_1 , and hence μ , via $(\mu - \mu_c)/k_B T = \ln(\bar{N}_1/N_1^{\text{coex}})$ [cf. Eq. (A18)], where $N_1^{\text{coex}} = (L^2 - \bar{l})n_1^{\text{coex}}$. Thus the average of several runs has to be taken, in order to obtain a meaningful accuracy. Figure 3 summarizes these averaged results for $2J/k_B T = 1.5$. At that temperature we have $\rho_G^{\text{coex}} = 3.11 \times 10^{-3}$ [cf. Eq. (A14)] and hence the factor $(1 - \rho_G^{\text{coex}}/\rho_L^{\text{coex}})$ may be neglected in Eqs. (30) and (32). Runs were made with $L = 25$ up to $L = 120$, with densities ρ in the range from about 1×10^{-2} up to 8×10^{-2} , which yielded average cluster sizes \bar{l} in the range from $\bar{l} = 26$ to $\bar{l} = 520$. Since for $\bar{l} \lesssim 100$ the

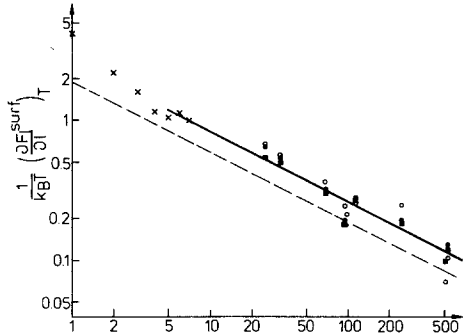


Fig. 3. Log-log plot of $(1/k_B T)(\partial F_i^{\text{surf}}/\partial l)_T$ vs l . Open dots are the results from the use of Eq. (47), while solid dots result from Eq. (32), and the crosses represent $\Delta F_i/k_B T$ as defined in Eq. (48). Dashed curve represents the capillarity approximation, Eq. (49). Solid squares represent the results of Eq. (32) corrected with Eq. (A31). The solid curve represents an estimate based on Eq. (52c).

expansion parameter $(\rho_G - \rho_G^{\text{coex}})/\rho_G^{\text{coex}}$ was not very small, we reinterpret Eq. (30) as follows:

$$\begin{aligned} \left. \left(\frac{\partial F_i^{\text{surf}}}{\partial l} \right)_{T, l^*} \right|_{l^*} &= \frac{\rho_G^{\text{coex}}}{\rho_G} \left(\frac{\rho_G}{\rho_G^{\text{coex}}} - 1 \right) \left[1 - \frac{1}{2} \left(\frac{\rho_G}{\rho_G^{\text{coex}}} - 1 \right) \right] \\ &\approx \frac{\rho_G^{\text{coex}}}{\chi_G} \ln \frac{\rho_G}{\rho_G^{\text{coex}}} \end{aligned} \quad (47)$$

by approximating the factor $C_G/\chi_G^2 - 1/\rho_L^{\text{coex}} \approx -1/\rho_G^{\text{coex}}$ and interpreting the resulting expression as the first two terms of the series expansion of $\ln(\rho/\rho_G^{\text{coex}})$. While this procedure may seem somewhat ambiguous, no such ambiguity arises when Eq. (32) is used, $\mu - \mu_c$ being determined as $k_B T \ln(\bar{n}_1/n_1^{\text{coex}})$ as noted above. Since $(\mu - \mu_c)/k_B T$ is not small for $\bar{l} \lesssim 100$, it would be very inaccurate to use the linear approximation $(\mu - \mu_c)/k_B T \approx (\bar{n}_1 - n_1^{\text{coex}})/n_1^{\text{coex}}$. Both ρ_G and \bar{n}_1 are observed in the simulations. In the ideal gas case, Eqs. (32) and (47) should yield identical results. Since the density of dimers at the coexistence curve $n_2^{\text{coex}} \ll n_1^{\text{coex}}$ (cf. the Appendix), and also the observed dimer density $\bar{n}_2 \ll \bar{n}_1$ is in fact observed in the simulations, we expect that the difference in $(\partial F_i^{\text{surf}}/\partial l)_{T, l^*}$, as determined from Eqs. (32) and (47) should not exceed the statistical errors. Figure 3 shows that this expectation is indeed correct. Since $(\mu - \mu_c)/k_B T$ is not very small in our case, we have to worry about a possible influence of the correction factor in Eq. (35). Calculating this correction from Eq. (A31), one obtains the solid squares rather than the solid circles in Fig. 3. Apart from the case $\bar{l} = 26$, this correction seems to be negligible in comparison with the statistical error.

The Monte Carlo results have been complemented at small l by using the series expansions for $n_l(\mu_c, T)$ described in the Appendix and by defining

$$\Delta F_l = \frac{1}{2}(F_{l+1}^{\text{surf}} - F_{l-1}^{\text{surf}}) \tag{48}$$

where the F_l^{surf} are calculated according to Eq. (A23). These estimates for $\Delta F_l/k_B T \approx (1/k_B T) \partial F_l^{\text{surf}}/\partial l$ are included in Fig. 3 for $l = 1, \dots, 7$. It is seen that the Monte Carlo data seem to extrapolate smoothly toward these values.

We also include the result for the capillarity approximation, Eq. (23), which yields in our case

$$\frac{1}{k_B T} \left(\frac{\partial F_l^{\text{surf}}}{\partial l} \right)_T = \pi^{1/2} \frac{f_s(T)}{k_B T} l^{-1/2} \approx 1.85 l^{-1/2} \tag{49}$$

where Eq. (A24) is used. It is seen that Eq. (49) yields values which are too small, at least for $l \leq 70$. This behavior is just opposite to what one would expect from Tolman-like corrections. The reason for this failure is obvious when we compare the cluster concentration n_l^{cap} that would follow from the use of Eqs. (23) and (A24) for the concentration of small clusters,

$$\begin{aligned} n_l^{\text{cap}} &\equiv \exp \left[-2(\pi l)^{1/2} \frac{f_s(T)}{k_B T} \right] \\ &\approx \exp \left[-\frac{4J(\pi l)^{1/2}}{k_B T} + 4(\pi l)^{1/2} e^{-2J/k_B T} \right] \\ &\approx \exp \left(-\frac{4J(\pi l)^{1/2}}{k_B T} \right) \left[1 + 4(\pi l)^{1/2} e^{-2J/k_B T} + O(e^{-4J/k_B T}) \right] \end{aligned} \tag{50}$$

with the low-temperature expansion, Eq. (A21), which we rewrite as

$$n_l = a_l \exp \left(-\frac{4Jx_l}{k_B T} \right) [1 + c_{1l} e^{-4J/k_B T} + O(e^{-8J/k_B T})] \tag{51}$$

First we note that $x_l > (l\pi)^{1/2}$ for all l (see Fig. 7); thus the capillarity approximation *underestimates* the actual surface energy of the clusters. Second we note that the leading corrections (due to surface entropy) are of order $e^{-4J/k_B T}$; no terms of order $e^{-2J/k_B T}$ enter. Thus the capillarity approximation *overestimates* the surface entropy. Both effects tend to make F_l^{surf} and hence also $(\partial F_l^{\text{surf}}/\partial l)_T|_l$ too small, as observed in Fig. 3.

Since we are dealing with a square lattice, we could think of improving on the capillarity approximation by not assuming clusters of circular shape as done in Eqs. (23), (49), and (50), but rather clusters whose shape is a square, the configuration of minimum energy on the lattice considered. This amounts to replacing the factor $\sqrt{\pi}$ in Eqs. (49) and (50) by a factor 2. However, even then one obtains from Eq. (50) the correct x_l for $l = 1, 4, 9$, only,

while still $x_l > (2l)^{1/2}$ for $l = 2, 3, 5, 6, 7, 8$, etc. Thus for many cluster sizes the minimum-energy configurations involve more broken bonds than expected in terms of an extrapolation from flat surfaces.

This conclusion is corroborated by a direct Monte Carlo study of the mean surface energy of clusters, which we obtain as a by-product of our study (Fig. 4). According to the capillarity approximation the surface energy at low temperatures should be given by

$$\bar{E}_l/4J = (\pi l)^{1/2} \tag{52a}$$

which again fails to reproduce correctly both the data and the low-temperature expansion results. But note that at the low temperatures studied here we have a relation $\bar{E}_l \propto l^{1/2}$ for $l \gtrsim 10$, as expected from previous work.⁽²⁶⁾ Indeed, our results only prove the capillarity approximation to be wrong if the bulk surface tension is used. With an effective surface tension fitted to the simulation results one finds reasonable agreement with the classical prediction $F_l^{\text{surf}} \propto l^{1/2}$ for $4 \leq l \leq 500$, as Figs. 3 and 4 show. This conclusion agrees with findings of Bauchspiess and Stauffer⁽⁴⁴⁾ on the simpler but much less realistic percolation model. But so far no simple and reliable prescription exists to calculate this "microscopic surface tension" from any bulk data.

The data of Fig. 4 can be used to estimate the coefficient $E_1(l)$ in the expansion

$$\bar{E}_l(T) = E_l(0)[1 + E_1(l)e^{-4J/k_B T} + O(e^{-8J/k_B T})] \tag{52b}$$

which in turn yields the leading term in the low-temperature expansion of F_l^{surf} , i.e.,

$$F_l^{\text{surf}}/k_B T = [E_l(0)/k_B T][1 - (k_B T/4J)E_1(l)e^{-4J/k_B T} + \dots] \tag{52c}$$

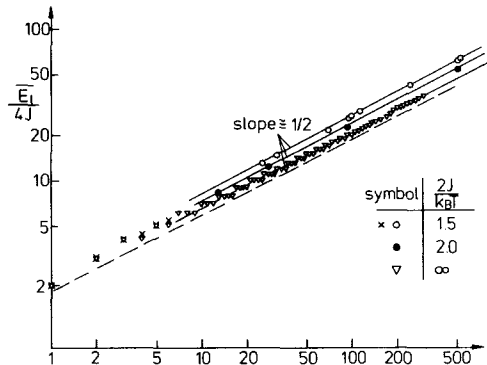


Fig. 4. Log-log plot of $\bar{E}_l/4J$ vs. l . Open and solid dots represent Monte Carlo results, while the crosses result from the series expansion (A21). The zero-temperature results (triangles) are the exact values of x_l in Eq. (A21). Dashed curve represents the capillarity approximation, Eq. (52).

The estimate for $(1/k_B T) \partial F_i^{\text{surf}} / \partial l$ that follows from Fig. 4 via Eq. (52c) is included as a solid line in Fig. 3. It is seen to be in much better agreement with the simulation data than is the capillarity approximation, Eq. (49). This fact proves the internal consistency of our data.

5. ANALYSIS OF THE CLUSTER DIFFUSIVITY

The exchange $\rho_i \rightarrow \rho_j, \rho_j \rightarrow \rho_i$ between neighboring sites in the lattice gas model leads to an effective “diffusion” of the clusters, i.e., their center of gravity performs some random walk. Of course, the diffusivity D_l of clusters (which measures the mean square displacement of the cluster center of gravity per unit time) decreases very strongly with cluster size. The diffusion and coagulation of clusters has been invoked as a mechanism of phase-separation kinetics.^(48,49) It has been suggested that D_l should follow a power law $D_l \propto l^{-y}$,⁽⁴⁹⁾ and various estimates for y have been made.^(46,48,49) Since the precise behavior of D_l has interesting consequences for these theories on phase separation kinetics,^(48,49) we estimate D_l from the Monte Carlo simulations. In a previous study⁽⁴⁵⁾ D_l was estimated from clusters which appeared in the course of the phase separation process and which continually changed size. As a consequence precise estimates of diffusivity were not possible. In the present case, where clusters are in equilibrium, there is no *net* change in cluster size, and a more accurate treatment is possible.

We first discuss the proposed mechanisms (Fig. 5). Binder and Stauffer⁽⁴⁹⁾ suggested that at low temperatures processes should dominate where an atom at the surface moves without energy cost (Fig. 5A) or evaporates with low energy cost (energy change $2J$) and reimpinges on the cluster surface again (Fig. 5B). In both cases the displacement of the cluster center of gravity is of order l^{-1} , and since a number $\propto l^{1-1/d}$ surface sites may participate in the process, we get a diffusivity (A_1 is a constant of order unity)^(48,49) $D_l \propto l^{-y_1}$, i.e.,

$$D_l = A_1 e^{-2J/k_B T} l^{1-1/d} (l^{-1})^2 = A_1 e^{-2J/k_B T} l^{-1-1/d} l^{-1}, \quad y_1 = 1 + 1/d \quad (53)$$

At higher temperatures two more mechanisms become important: if “gas” bubbles within the cluster move, one also produces displacements of the cluster center of gravity of order l^{-1} (Fig. 5C). A number of $n_1 l \approx e^{-8J/k_B T} l$ sites of the cluster participate in this process, and hence⁽⁴⁶⁾ (A_2 is another constant of order unity)

$$D_l = A_2 e^{-8J/k_B T} l (l^{-1})^2 = A_2 e^{-8J/k_B T} l^{-1}, \quad y_2 = 1 \quad (54)$$

This mechanism does not dominate asymptotically for large l , however, since another mechanism with still smaller y exists.⁴ Suppose that on one side of a

⁴ We are greatly indebted to J. Percus for a helpful discussion on this point.

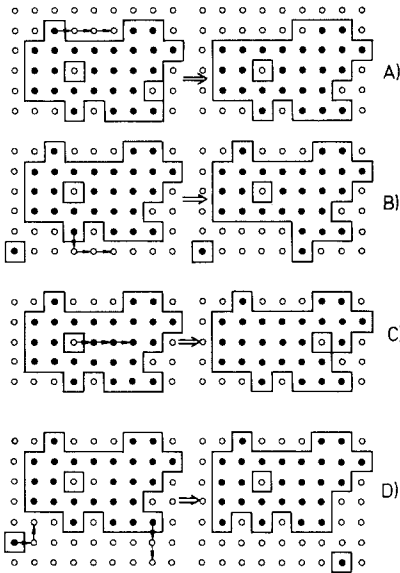


Fig. 5. Schematic illustration of four different mechanisms of cluster diffusion in a square lattice gas. For explanations see the text.

cluster an atom evaporates, while on the other side an atom condenses out of the gas phase on it (Fig. 5D). Now the displacement of the cluster center of gravity is of order $l^{1/d}/l = l^{-1+1/d}$; since the rate of this process is proportional to the gas density ($e^{-B/k_B T}$) and the number of surface sites ($\propto l^{1-1/d}$), we obtain (A_3 is another constant of order unity)

$$D_l = A_3 e^{-B/k_B T} l^{1-1/d} (l^{-1+1/d})^2 = A_3 e^{-8J/k_B T} l^{-1+1/d}, \quad y_3 = 1 - 1/d \quad (55)$$

While the rate described by Eq. (54) is generally small in comparison to that of Eq. (55), we expect some crossover between $y_1 = 1 + 1/d$ and $y_3 = 1 - 1/d$ due to the different temperature-dependent prefactors of Eqs. (55) and (53): For small l we expect D_l to be close to Eq. (53), since its prefactor is much larger at low temperatures, while Eq. (55) should dominate at large l . Hence on a log-log plot of D_l vs l one should observe an apparent exponent y_{eff} between these limits $1 - 1/d$ and $1 + 1/d$, and there should also be some variation of y_{eff} with temperature. Figure 6 shows that this expectation is indeed borne out. At first values of y_{eff} close to unity were interpreted⁽⁴⁶⁾ as evidence for Eq. (54). However, we now believe that the interpretation in terms of the crossover is correct. A simplified description of the crossover is obtained from Eqs. (53) and (55) as (A is a parameter independent of l)

$$D_l \approx A l^{-1-1/d} (1 + e^{-6J/k_B T} l) \quad (56)$$

Fitting A at both temperatures where calculations are available accounts for D_l in the crossover regime (Fig. 6) as well.

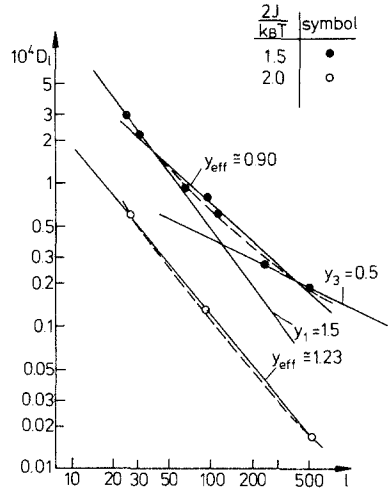


Fig. 6. Log-log plot of cluster diffusivity D_l vs l (time unit is one attempted exchange/site). Straight lines indicate various estimates for the exponent γ , while the dashed curves represent Eq. (56).

6. CONCLUSIONS

We summarize the main results of this investigation as follows:

(i) A cluster of size l (with $l^{1/d} \gg \xi$, the correlation length of density fluctuations) in a box V with constant total density can be in stable equilibrium with the surrounding gas for a suitable range of values l/V , although the equilibrium is unstable for $l/V \rightarrow 0$ (Section 2). Neglecting corrections of order $\exp(-V^{1/d}/\xi)$, which are very small in our case, quasimacroscopic thermodynamic considerations apply to describe the equilibrium. We find then that the equilibrium is precisely given in terms of the Kelvin equation (32) when one neglects the interaction forces between the cluster and surrounding gas, thus treating both cluster and gas as additive subsystems (but taking the excluded volume into account). The intuitive explanation for this absence of any l/V corrections is that the cluster has no “information” that the total system is finite when one neglects the $\exp(-V^{1/d}/\xi)$ corrections: thus the equilibrium condition remains the same, although the chemical potential μ now is not fixed but fluctuating in a finite system at constant average density.

(ii) A cluster definition where the gas atoms surrounding the cluster in the box are counted as being part of the cluster is analyzed in detail by our theory (Section 3). It is shown that an accurate estimate for F_N^{surf} can be obtained only if the gas density is smaller than 10^{-3} times the liquid density. Then this definition is preferable because it is very convenient to use. But it is suspected from our analysis that published surface free energies for argon clusters at $T = 84$ K may be in error by several percent, and hence it is

unclear to what extent conclusions regarding the validity of the Lothe–Pound theory are possible on the basis of these results.

(iii) Performing computer simulations of clusters in the two-dimensional lattice gas model, it is shown that our analysis (Section 2) in fact presents a helpful tool for their interpretation (Section 4). It is shown that the capillarity approximation *underestimates* the surface free energy of small clusters, in contrast to what one would expect from Tolman-like corrections. Performing approximate low-temperature expansions for the concentrations of very small clusters (Appendix), we show that this enhancement of the free energy of formation of small clusters is due to two sources: The use of the surface tension for flat surfaces tends to underestimate the number of “broken bonds,” i.e., the surface energy, and to overestimate the contributions of possible fluctuations, i.e., the surface entropy. We speculate that in real gas–fluid systems this enhancement of the cluster formation free energy due to the larger “microscopic surface tension” may be cancelled numerically to a large extent in many systems by the decrease of the cluster-formation free energy due to the Lothe–Pound translation–rotation corrections. Such an accidental cancellation could be the reason why the capillarity approximation describes nucleation well in many real systems (experiments of Katz *et al.*). In fact, in nucleation experiments close to T_c (where Lothe–Pound corrections are negligible due to the large size of the critical cluster) a dramatic failure of the capillarity approximation was observed, the cluster-formation free energies being distinctly larger, consistent with our treatment. It is expected that the “microscopic surface tension” decreases with increasing cluster size and may reach the macroscopic surface tension of a flat surface for cluster linear dimensions of about 10ξ , as suggested earlier by Binder and Stauffer. In this connection it is gratifying to note that very recently the surface tension of curved liquid surfaces has been measured directly, and was in fact larger than expected from the capillarity approximation.⁽⁵³⁾

(iv) As a by-product, the variation of the cluster diffusivity D_l with cluster size l is obtained (Section 5). It is shown that a crossover occurs from $D_l \propto l^{-1-1/d}$ at small l to $D_l \propto l^{-1+1/d}$ at large l ; the position of the crossover depends on temperature.

APPENDIX. STATISTICAL MECHANICS OF THE LATTICE GAS

In this appendix we summarize relations, most of which are well known;⁽⁴¹⁾ a coherent description of them is necessary to clarify the notation and make our analysis transparent for the reader. We start by considering the Ising Hamiltonian of a ferromagnet on a lattice (sites are labeled by index i),

$$\mathcal{H}_{\text{Ising}} = -J \sum_{\langle i, j \rangle} \sigma_i \sigma_j - H \sum_i \sigma_i, \quad \sigma_i = \pm 1 \quad (\text{A1})$$

where the symbol $\langle i, j \rangle$ means that all nearest neighbor pairs i, j are summed once. J is the exchange energy, and H is the magnetic field (measured in units

$g\mu_B = 1$). Since the Hamiltonian is invariant under the transformation $H \rightarrow -H, \{\sigma_i\} \rightarrow \{-\sigma_i\}$, the free energy has the symmetry

$$F(T, H) = F(T, -H) \tag{A2}$$

Due to the particle-hole symmetry of the lattice gas, Eq. (A2) leads to a relation between the free energies of “lattice gas” and “lattice fluid” phases. One obtains the lattice gas model from Eq. (A1) by introducing a local density variable $\rho_i (=0, 1)$ by

$$\sigma_i = 1 - 2\rho_i \tag{A3}$$

with which Eq. (1) is transformed into

$$\mathcal{H}_{\text{Ising}} = -\frac{1}{2}qJV - HV + (2H + 2qJ) \sum_i \rho_i - 4J \sum_{\langle i,j \rangle} \rho_i \rho_j \tag{A4}$$

In Eq. (A4), q denotes the coordination number of the lattice, which has V sites (i.e., we measure the volume in units of the elementary cell). From Eq. (A3) we may relate the magnetization/spin $M = \langle \sigma_i \rangle$ and density $\rho = \langle \rho_i \rangle = N/V$ as

$$M = 1 - 2\rho \tag{A5}$$

Now we consider the free energy $F_1(T, V, H)$ of the Ising magnet,

$$\begin{aligned} Z &\equiv \exp \frac{-F_1}{k_B T} = \text{Tr}_{\{\sigma_i = \pm 1\}} \exp \frac{-\mathcal{H}_1}{k_B T} \\ &= \exp \frac{1}{k_B T} \left(\frac{1}{2} qJV + HV \right) \text{Tr}_{\{\rho_i = 0, 1\}} \exp \left| -\frac{2H + 2qJ}{k_B T} \sum_i \rho_i \right| \\ &\quad \times \exp \left| \frac{4J}{k_B T} \sum_{\langle i,j \rangle} \rho_i \rho_j \right| \end{aligned} \tag{A6}$$

Since $N = \sum_i \rho_i$, we have to define the chemical potential μ of the lattice gas as

$$\mu = -2H - 2qJ = -2H + \mu_c, \quad \mu_c = -2qJ \tag{A7}$$

where μ_c is the chemical potential at the coexistence curve, and where we note that the coexistence between spin-up and spin-down magnetic phases (which occurs at $H = 0$) corresponds to the coexistence between the “lattice gas” and “lattice fluid” phases. Hence the free energy is rewritten as

$$\begin{aligned} \exp \frac{-F_1}{k_B T} &= \exp \left(\frac{\frac{1}{2}qJV + HV}{k_B T} \right) \sum_N \exp \left(\frac{N\mu}{k_B T} \right) \\ &\quad \times \text{Tr} \exp \left(\frac{2J}{k_B T} \sum_{\langle i,j \rangle} \rho_i \rho_j \right) \quad \{\rho_i = 0, 1 \text{ at fixed } N\} \\ &= \exp \left(\frac{\frac{1}{2}qJ + HV}{k_B T} \right) \sum_N \exp \left(\frac{N\mu}{k_B T} \right) Z_{\text{LG}}(N, V, T) \\ &= \exp \left(\frac{\frac{1}{2}qJ + HV}{k_B T} \right) \exp \left(-\frac{\Omega_{\text{LG}}}{k_B T} \right) \end{aligned} \tag{A8}$$

where Z_{LG} is the canonic partition function of the lattice gas, and $\Omega_{LG} = F_{LG} - \mu N$ its grand potential. Thus Eq. (A8) implies

$$F_1(T, H) = -\frac{1}{2}qJV - HV + \Omega_{LG}(T, V, \mu) \quad (\text{A9})$$

Since we may define $\Omega_{LF}(T, V, \mu)$

$$F_1(T, H < 0) = -\frac{1}{2}qJV + |H|V + \Omega_{LF}(T, V, \mu) \quad (\text{A10})$$

we find from Eqs. (A2), (A9) and (A10) that

$$\begin{aligned} \Omega_{LF}(T, V, \mu \geq \mu_c) &= -2HV + \Omega_{LG}(T, V, \mu \leq \mu_c) \\ &= (\mu - \mu_c)V + \Omega_{LG}(T, V, \mu \leq \mu_c) \end{aligned} \quad (\text{A11})$$

Since $\rho = -(1/V)(\partial\Omega/\partial\mu)_{T,V}$, we then have

$$\rho_L(T, \mu_c) = 1 - \rho_G(T, \mu_c), \quad \text{i.e.,} \quad \rho_L^{\text{coex}} = 1 - \rho_G^{\text{coex}} \quad (\text{A12})$$

Note that Eq. (A11) connects Ω_{LG} at some $\Delta\mu = \mu_c - \mu > 0$ with Ω_{LF} at $-\Delta\mu$; hence we have to reverse the sign when taking the derivative with respect to $\Delta\mu$. One finds furthermore from Eq. (A11) that

$$\chi_L = \chi_G, \quad C_L = -C_G \quad (\text{A13})$$

Hence it suffices to consider $\rho_G(T, \mu_c)$, χ_G , and C_G in the following. From Ref. 40 we note the exact series expansions in terms of the low-temperature variable $u = \exp(-4J/k_B T)$ for the square lattice

$$\rho_G^{\text{coex}} = u^2(1 + 4u + 17u^2 + 76u^3 + 357u^4 + 1736u^5 + 8659u^6 + \dots) \quad (\text{A14})$$

$$\begin{aligned} \chi_G &= (u^2/k_B T)(1 + 8u + 60u^2 + 416u^3 + 2791u^4 + 18,296u^5 \\ &\quad + 118,016u^6 + \dots) \end{aligned} \quad (\text{A15})$$

These expansions not only yield ρ_G^{coex} , χ_G with very high precision, but they also contain information on the low-temperature expansions for the concentrations $n_l(\mu_c, T)$ of clusters containing l spins for small l . This point is seen by generalizing the equation of state for an ideal lattice gas

$$\Omega_{LG}(T, V, \mu) = -k_B TV n_1(T, \mu) \quad (\text{A16})$$

where we denote the density of individual gas atoms ρ as "monomer density" n_1 , to an ideal mixture of clusters of various sizes l

$$\Omega_{LG}(T, V, \mu) = -k_B TV \sum_l n_l(T, \mu) \quad (\text{A17})$$

Since we assume the various clusters are in some kind of association-dissociation equilibrium with each other, a unique chemical potential μ rather than a whole set $\{\mu_l\}$ is sufficient. We now assume

$$n_l(\mu, T) = n_l(\mu_c, T) \exp[l(\mu - \mu_c)/k_B T] \quad (\text{A18})$$

in order to satisfy the relation

$$-(\partial\Omega_{LG}/\partial\mu)_{T,V} = V \sum_l l n_l(T, \mu) = N \quad (\text{A19})$$

which is an exact relation, if the clusters are defined in terms of “contours” around groups of atoms linked together via nearest neighbor bonds on the lattice.^(26,48) Hence we have the relations

$$\rho_G^{\text{coex}} = \sum_{i=1}^{\infty} l n_i(T, \mu_c), \quad \chi_G = \frac{1}{k_B T} \sum_{i=1}^{\infty} l^2 n_i(T, \mu_c) \quad (\text{A20})$$

In order to calculate the $n_i(T, \mu_c)$ we now introduce the low-temperature series expansions

$$n_i(T, \mu_c) = a_i u^{x_i} \left(1 + \sum_{k=1}^{\infty} c_{i,k} u^k \right) \quad (\text{A21})$$

Because of Eqs. (A14), (A15), (A20), and (A21) these coefficients $c_{i,k}$ should satisfy the sum rules ($c_{i,0} \equiv 1$)

$$\frac{1}{m!} \frac{\partial^m \rho_G^{\text{coex}}}{\partial u^m} \Big|_{u=0} = \sum_l a_l c_{l,m-x_l}, \quad \frac{1}{m!} \frac{\partial^m \chi_G}{\partial u^m} \Big|_{u=0} = \sum_l a_l l^2 c_{l,m-x_l} \quad (\text{A22})$$

where the sums run over all l consistent with the requirement $m \geq x_l$. We determine a_l, x_l by constructing the minimum-energy configuration for each cluster size (Fig. 7). For a mathematical discussion of this problem see Ref. 50. In order to use Eq. (A21) we finally have to determine the coefficients $c_{i,k}$. Constructing low-temperature expansions for higher derivatives of $\Omega_{LG}(T, V, \mu)$ with respect to μ , one would get additional sum rules from Eq. (A18). However, it would be impossible to take all these sum rules consistently into account, since Eq. (A17) is not exact (see also Ref. 51). Since ρ_G^{coex} and χ_G are the most relevant quantities in our thermodynamic treatment in Section 2, it is reasonable to construct “effective” cluster concentrations

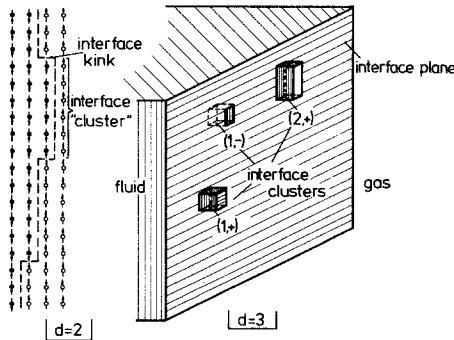


Fig. 7. Minimum-energy configurations for clusters in the lattice gas model. While for $l \leq 4$ all a_l geometrically distinct configurations are shown, only one configuration is shown for $l = 5, 6, 7$. Note that the number of broken bonds is $2x_l$.

$n_i(T, \mu_c)$ which fit ρ_G^{coex} and χ_G . In order to treat all cluster sizes with comparable accuracy, we cut off the summation in Eq. (A21) for $k > 2$, which is a good approximation since $u \rightarrow 0$ as $T \rightarrow 0$. From Eqs. (A14), (A15), (A21), and (A22) we then immediately find $c_{11} = c_{12} = 0$, $c_{21} = -5/4$. For $m = 5$ an ambiguity arises since both $x_3 = x_4 = 4$ (Fig. 7). We then assume that the correction c_{41} is solely due to the contribution of the less compact clusters with $l = 4$, and 10 broken bonds (10 clusters of which exist). Hence $a_4 = 10$, and thus $c_{31} = 8/9$, $c_{22} = -8$. Similarly, from $c_{51} = 13/4$, $c_{61} = 18$ we find $c_{32} = -8$, $c_{42} = -21/2$. Having thus obtained a truncated series for the $n_i(T, \mu_c)$, we then obtain from Eq. (A21) the cluster free energy F_i^{surf} via the definition

$$F_i^{\text{surf}}(\mu_c, T) = -k_B T \ln n_i(T, \mu_c) \quad (\text{A23})$$

Next we consider the interface free energy $f_s(T, \mu)$. From the exact solution⁽³³⁾ we have

$$f_s(\mu_c, T) = 2J - k_B T \ln \frac{1 + \sqrt{u}}{1 - \sqrt{u}} \approx 2J - 2k_B T e^{-2J/k_B T} + O(e^{-4J/k_B T}) \quad (\text{A24})$$

While the term $2J$ is the interface (free) energy at $T = 0$ where the interface is perfectly flat, the term $-2k_B T e^{-2J/k_B T}$ can be considered as the ideal gas law for "kinks" in the interface (Fig. 8). Each kink requires an excitation energy $2J$, and may go either to the right or to the left (thus we have a factor 2). Hence $f_s(\mu_c, T) \approx 2J + f_{\text{kinks}} = 2J - 2k_B T \rho_{\text{kink}}$, defining an effective kink density $\rho_{\text{kink}} = \exp(-2J/k_B T)$. In the three-dimensional simple cubic lattice, the interface is two dimensional and the excitations dominating at low temperatures are not "steps" but rather small isolated clusters (Fig. 8). This difference is due to the fact that the interface for $d = 2$ is rough at all $T > 0$, while it is not rough for $d = 3$ and low enough temperatures.⁽⁵²⁾ For $d = 3$ and $T \rightarrow 0$ the leading term is then, denoting monomers at the right of the interface as $n_1^+(\mu, T)$ and monomers at the left as $n_1^-(\mu, T)$,

$$\begin{aligned} f_s(\mu, T) &= 2J - k_B T [n_1^+(\mu, T) + n_1^-(\mu, T)] \\ &= 2J - 2k_B T e^{-8J/k_B T} \cosh \frac{\mu - \mu_c}{2k_B T} \end{aligned} \quad (\text{A25})$$

and hence we find that for $T \rightarrow 0$ and $\mu \rightarrow \mu_c$

$$\left(\frac{\partial f_s(\mu, T)}{\partial \mu} \right)_T \approx -\frac{\mu - \mu_c}{2k_B T} e^{-8J/k_B T} \quad (\text{A26})$$

which leads to Eq. (36). In two dimensions a low-temperature expansion of this type does not exist, since the interface is rough for all $T > 0$. Since the energy of single kinks would be infinite for $\mu \neq \mu_c$, we may treat two succes-

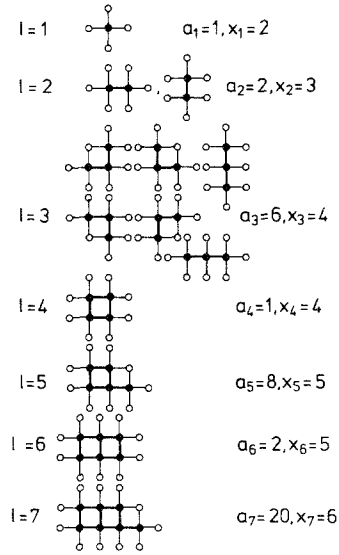


Fig. 8. Typical interface configurations at low temperatures for both $d = 2$ and $d = 3$, showing typical fluctuations: kinks ($d = 2$) and clusters, either to the right (+) or left (-) of the interface.

sive kinks going into opposite direction as a “cluster.” Since the density of kinks goes to zero at $T \rightarrow 0$, the typical sizes \bar{l} of these “clusters” becomes very large. Hence we may write approximately for $d = 2$

$$\begin{aligned}
 f_s(\mu, T) &\approx 2J - 2k_B T \sum_l n_l(\mu_c, T) \cosh\left(l \frac{\mu - \mu_c}{2k_B T}\right) \\
 &\approx 2J - 2k_B T \int dl n_l(\mu_c, T) \cosh\left(l \frac{\mu - \mu_c}{2k_B T}\right) \\
 &\approx 2J - 2k_B T \bar{l} n_l(\mu_c, T) \cosh\left(\bar{l} \frac{\mu - \mu_c}{2k_B T}\right) \quad (A27)
 \end{aligned}$$

We note that $n_l(\mu_c, T) = e^{-4J/k_B T}$, independent of l , since two kinks are involved. Since $\bar{l} \approx \exp(2J/k_B T)$, the inverse of the kink density ρ_{kink} , we obtain

$$f_s(\mu, T) \approx 2J - 2k_B T e^{-2J/k_B T} \cosh\left(e^{2J/k_B T} \frac{\mu - \mu_c}{2k_B T}\right) \quad (A28)$$

which is only roughly correct due to the approximation in Eq. (A27), but reduces to the correct equation (A24) for $\mu = \mu_c$. Hence we expect that

$$\left(\frac{\partial f_s(\mu, T)}{\partial \mu}\right)_T \approx -\frac{\mu - \mu_c}{2k_B T} e^{2J/k_B T} \quad (A29)$$

apart from factors of order unity in which we are not interested. Equation (A29) again leads to Eq. (36).

Equation (A29) implies a divergence of the "surface" susceptibility χ_s in Eq. (36) as $T \rightarrow 0$, and hence the contribution of this term must be treated with care. However, we think that the treatment in Eqs. (A27)–(A29), which is appropriate for a flat interface, substantially overestimates χ_s for a small cluster. In fact, the limited interface of a small cluster does not allow it to have interface kinks widely separated from each other as implied by $\bar{l} \approx \exp(2J/k_B T)$ used above, but again only rather small "interface clusters" may be formed as in the three-dimensional case. Thus we assume that for small clusters we should use in Eq. (27) the term with $l = 1$ only, which yields

$$\left(\frac{\partial f_s^{\text{eff}}(\mu, T)}{\partial \mu}\right)_T \approx -\frac{\mu - \mu_c}{2k_B T} e^{-4J/k_B T} \quad (\text{A30})$$

which is a result analogous to Eq. (A26). Using Eq. (A30) in Eq. (35) yields finally

$$\left(\frac{\partial F_i^{\text{surf}}}{\partial l}\right)_T = \left(\frac{\partial F_i^{\text{surf}}}{\partial l}\right)_{T,u} \left(1 + \frac{\mu - \mu_c}{k_B T} \frac{l}{V} \frac{e^{-4J/k_B T}}{(2J/k_B T)\chi_G}\right) \quad (\text{A31})$$

ACKNOWLEDGMENTS

We thank J. K. Percus for a valuable conversation about cluster diffusivity mechanisms and H. Müller-Krumbhaar and D. Stauffer for valuable comments and careful reading of the manuscript.

REFERENCES

1. (a) A. C. Zettlemoyer, ed., *Nucleation* (Marcel Dekker, New York, 1969); (b) A. C. Zettlemoyer, ed., *Nucleation Phenomena* (Elsevier, New York, 1977); esp. articles by H. Reiss, p. 1, and R. Kikuchi, p. 67.
2. F. H. Stillinger, *J. Chem. Phys.* **38**:1486 (1963).
3. J. J. Burton, in *Statistical Mechanics, Modern Theoretical Chemistry, Vol. 5*, V. J. Berne, ed. (Plenum, New York, 1977).
4. F. F. Abraham, *Homogeneous Nucleation Theory* (Academic Press, New York, 1974).
5. K. Binder and D. Stauffer, *Adv. Phys.* **25**:343 (1976).
6. J. L. Katz, C. J. Scoppa, N. G. Kumar, and P. Mirabel, *J. Chem. Phys.* **62**:448 (1975); see also G. M. Point, *Nat. Bur. Std. (U.S.), J. Phys. Chem. Ref. Data* **1**:119 (1972); J. L. Katz, C. J. Scoppa, N. G. Kumar, and P. Mirabel, *Disc. Faraday Soc.* **61**:83 (1976).
7. A. W. Castleman, Jr., Nucleation and molecular clustering about ions, Univ. Colorado preprint; A. W. Castleman, Jr., P. M. Holland, and R. G. Keesee, *J. Chem. Phys.* (1978), in press.
8. R. B. Heady and J. W. Cahn, *J. Chem. Phys.* **58**:896 (1973).
9. J. S. Huang, W. I. Goldberg, and M. R. Moldover, *Phys. Rev. Lett.* **34**:639 (1975); W. I. Goldberg and J. S. Huang, in *Physics of Nonequilibrium Systems*, T. Riste, ed. (Plenum Press, New York, 1975), p. 87.

10. R. C. Tolman, *J. Chem. Phys.* **17**:118, 333 (1949).
11. J. G. Kirkwood and F. P. Buff, *J. Chem. Phys.* **17**:338 (1949).
12. L. Dufour and R. Defay, *Thermodynamics of Clouds* (Academic Press, New York, 1963).
13. J. Lothe and G. M. Pound, *J. Chem. Phys.* **38**:2080 (1962).
14. J. Feder, K. C. Russell, J. Lothe, and G. M. Pound, *Adv. Phys.* **15**:117 (1966).
15. J. W. Cahn and J. E. Hilliard, *J. Chem. Phys.* **28**:258 (1958); **31**:688 (1959).
16. K. W. Sarkies and N. E. Frankel, *J. Chem. Phys.* **54**:433 (1971); *Phys. Rev. A* **11**:1724 (1975).
17. J. S. Langer and L. A. Turski, *Phys. Rev. A* **8**:3230 (1973); K. Kawasaki, *J. Stat. Phys.* **12**:365 (1975).
18. C. S. Kiang and D. Stauffer, in Ref. 1b; see also C. S. Kiang and D. Stauffer, *Z. Phys.* **235**:130 (1970).
19. M. E. Fisher, *Physics* **3**:255 (1967).
20. A. Eggington, C. S. Kiang, D. Stauffer, and G. H. Walker, *Phys. Rev. Lett.* **26**:820 (1971); C. S. Kiang, D. Stauffer, G. H. Walker, O. P. Puri, T. D. Wise, Jr., and E. M. Patterson, *J. Atmos. Sci.* **28**:1112 (1971).
21. P. Hamill, C. S. Kiang, and D. Stauffer, *Chem. Phys.* **28**:209 (1974).
22. H. P. Gillis, D. C. Marvin, and H. Reiss, *J. Chem. Phys.* **66**:214, 223 (1977).
23. M. R. Hoare and P. Pal, *Adv. Phys.* **24**:645 (1975).
24. J. J. Burton, *Acta Met.* **21**:1255 (1973).
25. E. Stoll, K. Binder, and T. Schneider, *Phys. Rev. B* **6**:2777 (1972); H. Müller-Krumbhaar, *Phys. Lett. A* **48**:459 (1974); A. Sur, J. L. Lebowitz, J. Marro, and M. H. Kalos, *Phys. Rev. B* **15**:3014 (1977).
26. K. Binder and D. Stauffer, *J. Stat. Phys.* **6**:49 (1972); K. Binder, *Ann. Phys.* **98**:390 (1976).
27. H. Reiss, J. L. Katz, and E. R. Cohen, *J. Chem. Phys.* **48**:5553 (1968).
28. J. K. Lee, J. A. Barker, and F. F. Abraham, *J. Chem. Phys.* **58**:3166 (1973); F. F. Abraham, *J. Chem. Phys.* **61**:1221 (1974).
29. D. J. McGinty, *J. Chem. Phys.* **58**:4733 (1973).
30. K. Binder, *J. Chem. Phys.* **63**:2265 (1975).
31. M. Rao, B. J. Berne, and M. H. Kalos, *J. Chem. Phys.* **68**:1325 (1978).
32. K. Binder, P. Miold, and M. H. Kalos, *Le Vide* **185** (Suppl.):112 (1977).
33. L. Onsager, *Phys. Rev.* **65**:117 (1944).
34. T. L. Hill, *Thermodynamics of Small Systems* (Benjamin, New York, 1963/1964).
35. M. E. Fisher, in *Critical Phenomena*, M. S. Green, ed. (Academic, New York, 1971).
36. K. Binder and D. P. Landau, *Surf. Sci.* **61**:577 (1976).
37. H. Müller-Krumbhaar, in *Current Topics in Materials Science, Vol. 1*, E. Kaldis, ed. (North-Holland, Amsterdam, 1978), p. 1.
38. K. Binder, in Ref. 1b, p. 279.
39. C. N. Yang, *Phys. Rev.* **85**:809 (1952).
40. C. Domb, in *Phase Transitions and Critical Phenomena, Vol. 3*, C. Domb and M. S. Green, eds. (Academic, New York, 1974), p. 357.
41. C. N. Yang and T. D. Lee, *Phys. Rev.* **87**:404 (1952); K. Huang, *Statistical Mechanics* (Wiley, New York, 1963).
42. K. Kawasaki, in *Phase Transitions and Critical Phenomena, Vol. 2*, C. Domb and M. S. Green, eds. (Academic, New York, 1972).
43. K. Binder, ed., *Monte Carlo Methods in Statistical Physics* (Springer, Berlin, 1978).
44. K. R. Bauchspiess and D. Stauffer, *J. Aerosol Sci.* (1978).
45. A. B. Bortz, M. H. Kalos, J. L. Lebowitz, and M. A. Zendejas, *Phys. Rev. B* **10**:535

- (1974); J. Marro, A. B. Bortz, M. H. Kalos, and J. L. Lebowitz, *Phys. Rev. B* **12**:2000 (1975); A. Sur *et al.*, Ref. 25.
46. M. Rao, M. H. Kalos, J. L. Lebowitz, and J. Marro, *Phys. Rev. B* **13**:7325 (1976); M. Rao, M. H. Kalos, J. L. Lebowitz, and J. Marro, in *Computer Simulation for Materials Applications*; R. J. Arsenault, J. R. Beeler, and J. A. Simmons, eds. (NBS, Geithersburg, Md., 1976), p. 180.
47. J. Marro, J. L. Lebowitz, and M. H. Kalos, preprint; M. H. Kalos, J. L. Lebowitz, O. Penrose, and A. Sur, *J. Stat. Phys.* **18**:39 (1978); O. Penrose, J. L. Lebowitz, J. Marro, M. H. Kalos, and A. Sur, *J. Stat. Phys.* **19**:243 (1978).
48. K. Binder, D. Stauffer, and H. Müller-Krumbhaar, *Phys. Rev. B* **12**:5261 (1975); K. Binder, *Phys. Rev. B* **15**:4425 (1977).
49. K. Binder and D. Stauffer, *Phys. Rev. Lett.* **33**:1006 (1974); P. Mirolid and K. Binder, *Acta Met.* **25**:1435 (1977); K. Binder, C. Billotet, and P. Mirolid, *Z. Phys. B* **30**:183 (1978).
50. F. Harary and H. Harborth, *J. Comb. Inf. Syst. Sci.* **1**:1 (1976).
51. M. F. Sykes and D. J. Gaunt, *J. Phys. A* **9**:2131 (1976).
52. G. Gallavotti, *Nuovo Cimento* **2**:133 (1972).
53. L. R. Fisher and J. N. Israelachviti, *Nature* **277**:548 (1979).